CarbonSAFE Phase II: 8.1.a Project ECO_2S Numerical Modeling Report

DOE Project DE-FE0029465

Submitted by:
Advanced Resources International, Inc.
4501 Fairfax Drive, Suite 910
Arlington, VA 22203

Principal Investigator:
George J. Koperna, Vice President
Advanced Resources International, Inc.
Phone: (703) 528-8420
Fax: (703) 528-0439
E-Mail: gkoperna@adv-res.com

Submitted to:
U.S. Department of Energy
National Energy Technology Laboratory

June 30, 2020

Disclaimers

U.S. Department of Energy

This report was prepared as an account of work sponsored by an agency of the United States Government. Neither the United States Government nor any agency thereof, nor any of their employees, makes any warranty, express or implied, or assumes any legal liability or responsibility for the accuracy, completeness, or usefulness of any information, apparatus, product, or process disclosed, or represents that its use would not infringe privately owned rights. Reference herein to any specific commercial product, process, or service by trade name, trademark, manufacturer, or otherwise does not necessarily constitute or imply its endorsement, recommendation, or favoring by the United States Government or any agency thereof. The views and opinions of authors expressed herein do not necessarily state or reflect those of the United States Government or any agency thereof.

Advanced Resources International, Inc.

The material presented in this report is intended to support the objectives of this specific Application only. Any use of this material in relation to any other specific application should be based on independent examination and verification of its unrestricted applicability for such use and on a determination of suitability for the application by professionally qualified personnel. No license under any Advanced Resources International, Inc., patents or other proprietary interest is implied by the publication of this Application. Those making use of or relying upon the material presented in this application for any other purpose, assume all risks and liability arising from such use or reliance.

Executive Summary

This report summarizes a reservoir simulation study on the CarbonSAFE Project ECO_2S Kemper Regional Storage Complex to understand how it can be developed and operated to accept a yearly volume of 22.5 million metric tons of carbon dioxide, captured and transported from three power plants. These sources are the gas-filled units of Plant Ratcliffe (with 0.7 MMmt of annual carbon dioxide emissions) and Plant Daniel (3.0 MMmt/yr), and the coal-fired units of Plant Miller (18.8 MMmt/yr), totaling 22.5 MMmt/yr of carbon dioxide or 675 MMmt over 30 years.

With such a significant volume of CO_2, this effort centered on how the plume would develop and how it may migrate, based on the current geological understanding. Of further interest was whether the plume size and direction could be minimized and/or more quickly immobilized through active plume management using water cycling techniques. A base simulation model was developed utilizing the latest geological interpretation of the saline storage formations, the Lower Tuscaloosa Massive sand, the Washita-Fredericksburg Dantzler and 'Big Fred' intervals, and the Paluxy. The data collected from the three Phase II wells were incorporated in the geological model for further refinement within the project site. Porosity-permeability transform functions were developed for these groups of reservoirs using log and core data.

The base model contains 21 carbon dioxide injection wells, located on seven well pads. Each well on a given pad is perforated in only one reservoir group, Massive sand/Dantzler (combined), Big Fred, or Paluxy zones. In other words, each reservoir group receives carbon dioxide through seven injection wells. If the total carbon dioxide daily injection rate were uniformly distributed among the three reservoir groups, the resulting carbon dioxide plume would be vastly different due to differences in rock properties, salinity, reservoir temperature and pressure. To get similar plume extents, different injection volumes were selected for each reservoir group. This arrangement resulted in the Massive sand formation getting the least and the Paluxy formations the most injection volume. The final carbon dioxide plume extent was approximately 55 square miles, which was developed at the top of the Massive sand, 30 years after the end of injection.

Sensitivity analysis on horizontal permeability anisotropy and hysteresis trapping gas saturation shows their impact on the plume size, changing it by as much as 27% over the base model assumptions, 30 years after the end of CO_2 injection. Water cycling was also studied in this model to see its impact on controlling the plume migration. Placement of water injection and production wells at a distance from the carbon dioxide injection wells and at different sides of the site were tested. Twelve water production wells (four assigned to each reservoir group) placed on four well pads would each extract 20,000 bbl/day of water. Twelve injection wells then re-inject the produced water through another part of the reservoir. A water cycling scenario, with the injectors on the up-dip of the formation and producers on the down-dip, that starts at the same time as the carbon dioxide injection and continues 30 years after the end of carbon dioxide injection could reduce the plume size by 18%.

Table of Contents

List of Figures

List of Tables

1.0 Introduction

In support of the USDOE-NETL CarbonSAFE *Project ECO₂S* effort, the Kemper Regional Storage Complex was characterized to assess its ability to store commercial volumes of CO_2 safely and securely (at least 50 million metric tons, MMmt) over a 30-year period. Adjacent to Plant Ratcliffe in central Mississippi, **Figure 1**, three wells were drilled in 2017 to provide a preliminary description of the subsurface geology for a 30,000-acre storage complex. The results of this characterization of three significant saline reservoirs have indicated that the storage complex's geologic properties are exceptional, with more than 1,100 feet of net sand, mean reservoir porosity of 28 percent, and a mean permeability of 3,500 mD. Applying the DOE storage efficiency factors for cases where site-specific reservoir data are available (Goodman et al., 2011) suggests a CO_2 storage capacity of approximately one gigatonne (Riestenberg et al., 2018). As a result, the storage complex appears more than capable of storing 50 MMmt of CO_2 and could serve as a regional storage hub where considerably more CO_2 volumes could be stored.

Southern Company, a project partner for this large-scale demonstration project, has a significant CO_2 footprint within approximately 150 miles of this storage complex, well within pipeline reach. These sources are the gas-fired units of Plant Ratcliffe (with 0.7 MMmt of annual CO_2 emissions), Plant Daniel (3.0 MMmt/yr) and the coal-fired units of Plant Miller (18.8 MMmt/yr), totaling 22.5 MMmt/yr of CO_2 or 675 MMmt over 30 years[1]. The Commercial Development Plan (Deliverable 8.2) provides details on the Kemper Regional Storage Complex regional storage potential.

[1] Assuming 90% capture.

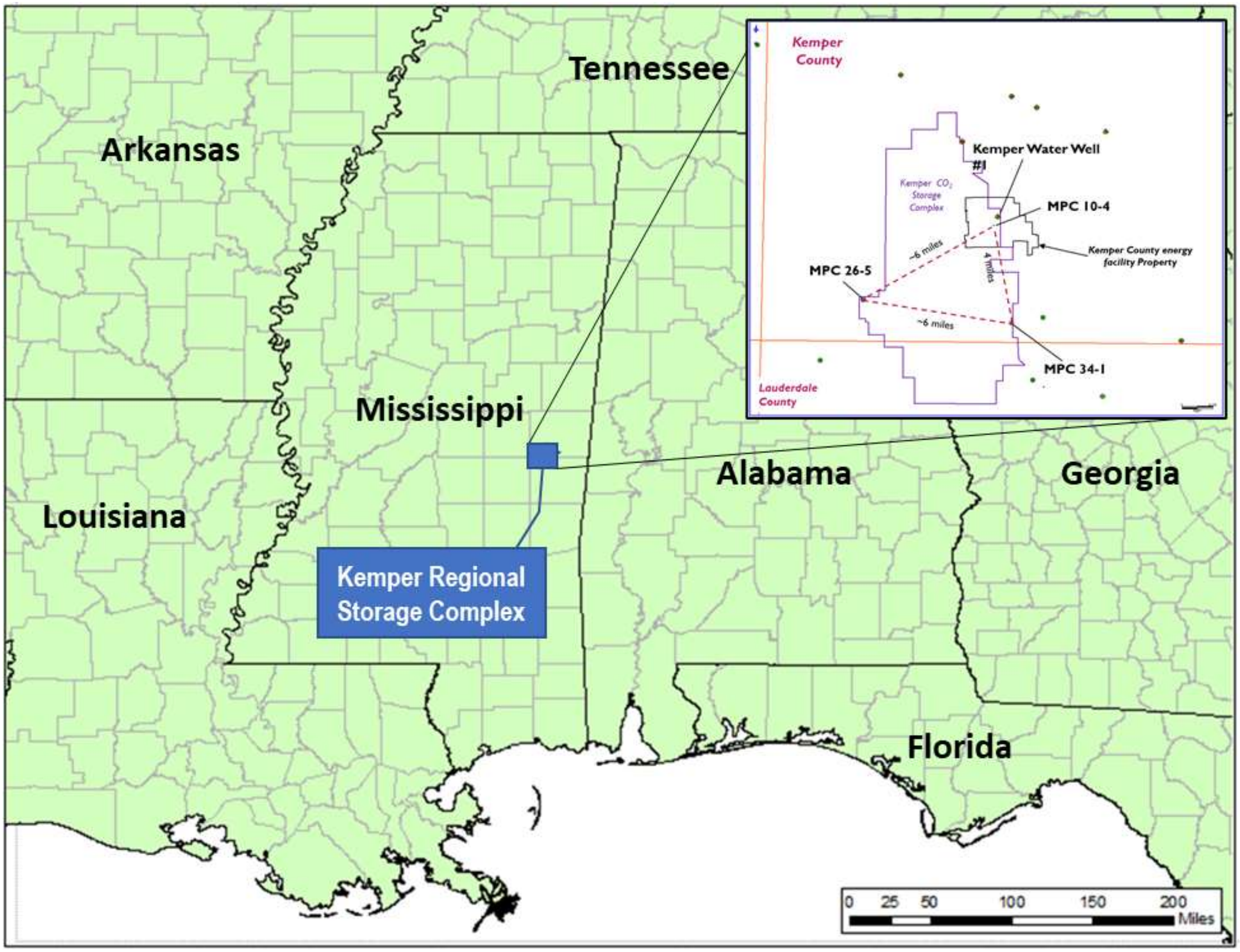

Figure 1: Kemper Regional Storage Complex location in Kemper County Mississippi.

This report summarizes a reservoir simulation study performed to understand how the Kemper Storage Complex could be developed and operated to accept 22.5 MMmt/yr of CO_2 from these three plants. With such a significant volume of CO_2, this effort centered about how the plume would develop and how it may migrate, based on the current geological understanding. Of further interest was whether the plume size and direction could be minimized and/or more quickly immobilized through active plume management using water cycling techniques.

The plume areal extent, calculated from the largest plume in the three target reservoirs, without any alteration strategies, is approximately 55 square miles 30 years after the end of CO_2 injection. The CO_2 plume migration path is up-dip to the northeast. A summary of the outcomes of base model and sensitivity cases is provided in **Table 1**.

Table 1: Summary of the Kemper reservoir simulation results

Model Description	Results
Base model	Largest plume size is 55 square miles
Horizontal permeability anisotropy	Absence of horizontal permeability anisotropy will result in a 27% larger plume
Hysteresis residual gas saturation	Increasing this parameter from 5% to 40% impacts the plume size by 5%
Water cycling with water injectors fully perforated in target reservoirs	Reduces plume size by 18%
Reduce water injector perforation interval	If partially perforated (only the top 100 feet), the plume is reduced by 10%
Water cycling placement	Placing water injectors up-dip of CO_2 wells (northeast), and water producers down-dip (southwest), the plume is reduced by 18%
Distance between water cycling and CO_2 injection wells	5-mile distance is selected over 2- and 3-mile distance due to CO_2 breakthrough

2.0 Kemper Regional Storage Complex Geology

2.1 Site Geology

Multiple saline reservoirs have the potential for large volume CO_2 storage within the Kemper Regional Storage Complex: the Paluxy Formation, the middle Washita-Fredericksburg interval 'Big Fred' interval (informal name), the upper Washita-Fredericksburg interval Dantzler sand, and the Lower Tuscaloosa Formation Massive sand, listed in ascending stratigraphic order (**Figure 2**). These formations are briefly described below. Thicknesses for each of the target saline reservoirs are shown in **Figure 3**.

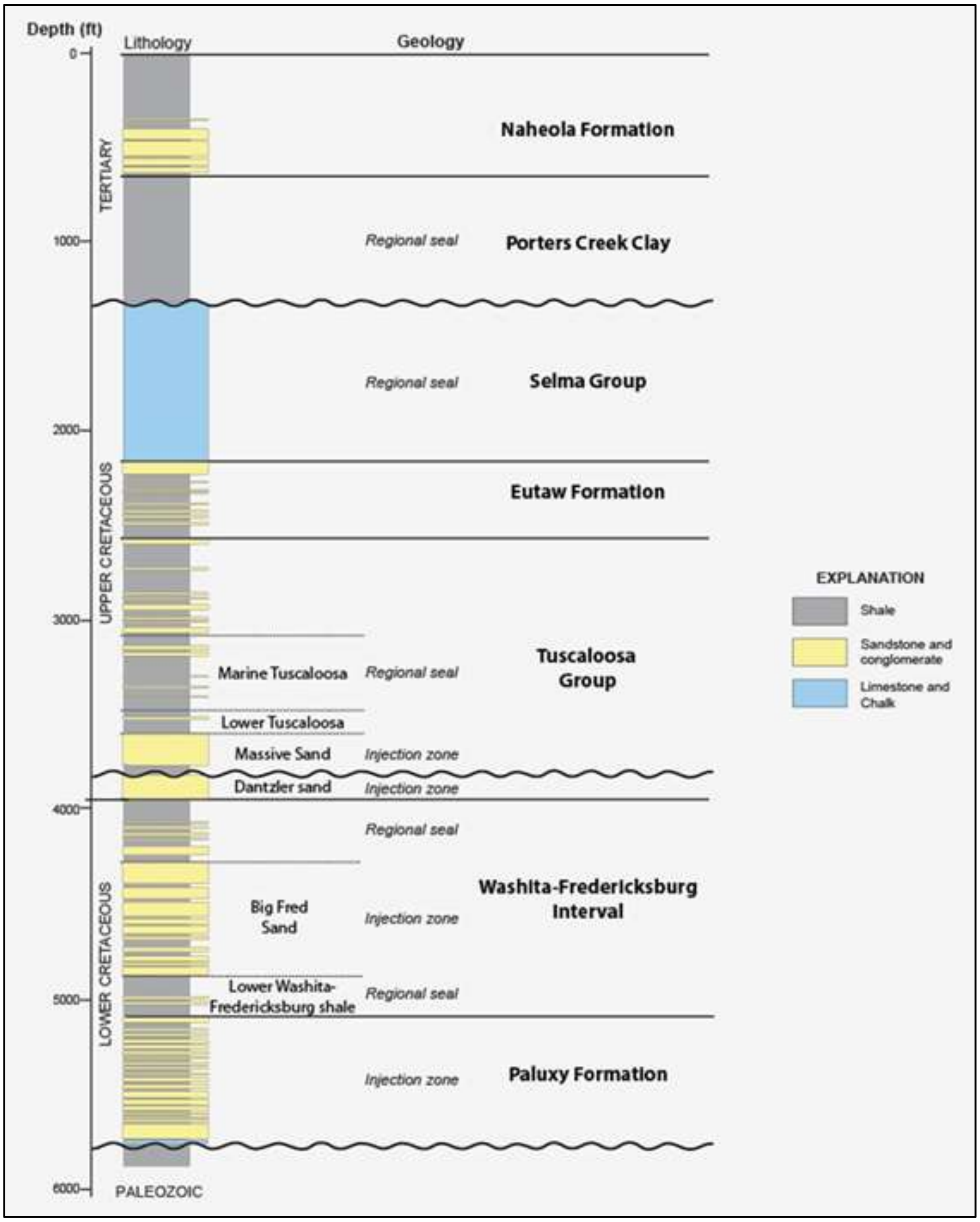

Figure 2: Kemper Regional Storage Complex Stratigraphic Column

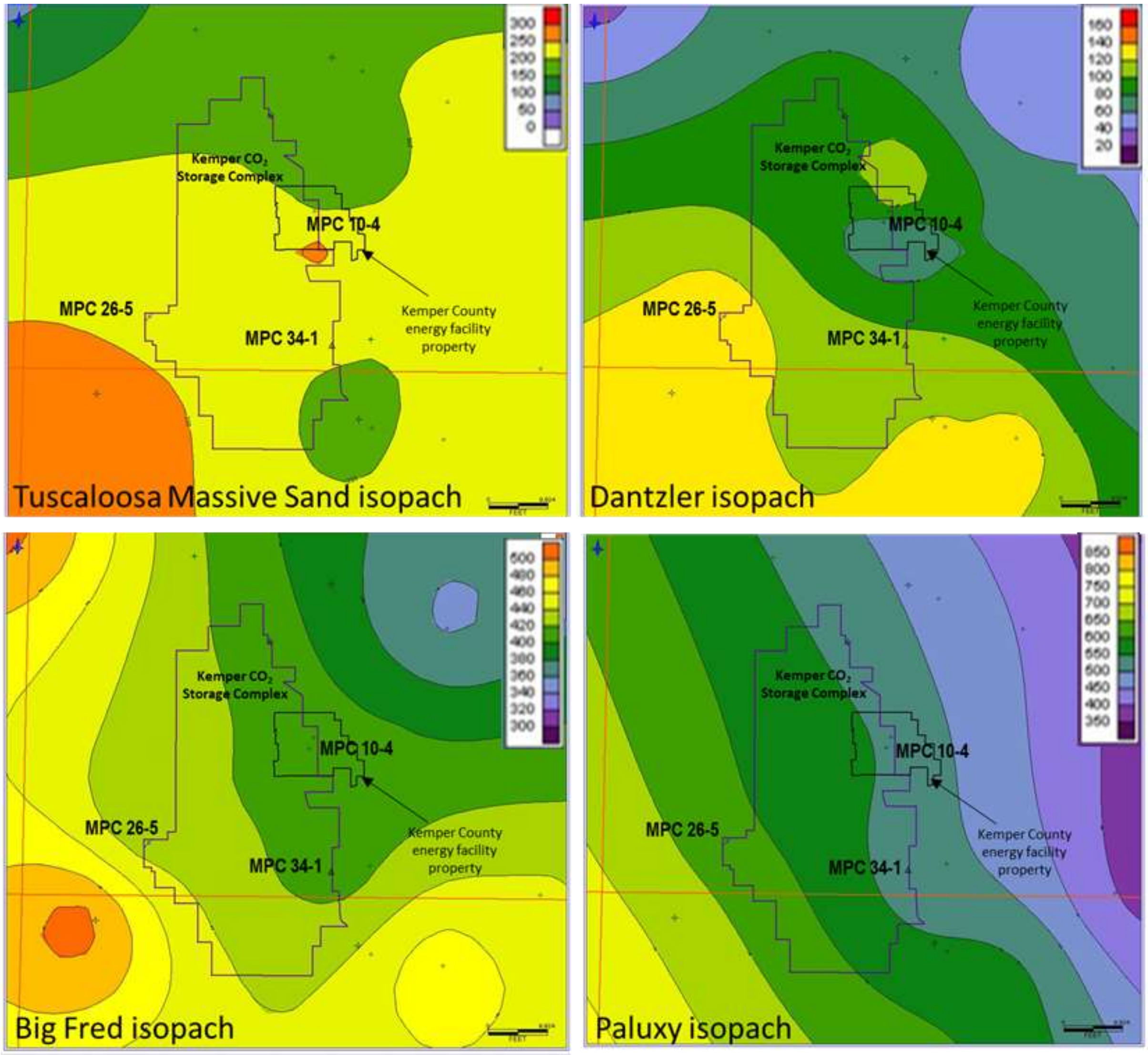

Figure 3: Isopach map of the total thickness of the Tuscaloosa Massive sand, Dantzler and "Big Fred" unit of the Washita-Fredericksburg Group and the Paluxy formation.

Paluxy Formation: The Paluxy Formation is approximately 558 feet thick at the *Project ECO₂S* test site. Paluxy strata are dominated by reservoir-quality sandstone and intervening shale units. The sandstone beds typically range in thickness from 10 to 98 feet whereas the shale interbeds are generally thinner than 20 feet. Multistory sand packages, interpreted as bedload-dominated fluvial sands (Pashin et al., AAPG 2018), can be correlated between wells, but the data coverage is not extensive enough to correlate individual sands. A prominent shale interval exists at the base of the Washita-Fredericksburg, which serves as a confining zone isolating the Paluxy Formation from the overlying Washita-Fredericksburg.

Washita-Fredericksburg Interval: The Washita-Fredericksburg interval is approximately 1,237 feet thick at the storage complex (**Table 2**). The group contains principally sandstone with lesser amounts of conglomerate and shale. At the top of the Washita-Fredericksburg interval is an informal (drillers) unit called the Dantzler sand. The central section, informally named the “Big Fred” sand, is composed of more than 90 percent sandstone and can approach a thickness of 427 feet. Like the Paluxy, the Washita-Fredericksburg interval is interpreted to contain bedload-dominated fluvial deposits. Internal shale breaks (baffles) are not significant features in the “Big Fred”. A thick and laterally extensive shale interval, which can range from 164 to 558 feet thick, exists at the upper section of the Washita-Fredericksburg and serves as a confining zone isolating the “Big Fred” interval from the overlying Dantzler unit and Massive sand reservoirs (**Figure 2**).

Lower Tuscaloosa Massive Sand: The Tuscaloosa Group is typically subdivided into three units in the region: (1) the lower Tuscaloosa Formation, (2) the Marine Tuscaloosa shale, and (3) the upper Tuscaloosa. The basal unit of the lower Tuscaloosa Group is referred to as the Massive sand, the shallowest storage reservoir in the Storage Complex, which is approximately 220 feet at the Kemper Storage Complex (**Table 2**). The Massive sand and the Dantzler can be treated as a single injection target as they are in close proximity, with a relatively thin shale break in between 20 and 49 feet in the storage complex. The depositional environment for the Massive sand is interpreted as fluvial to coastal in origin at the Kemper site (Mancini et al., 1987) and a laterally extensive reservoir is expected.

Table 2: Net to Gross for the target intervals in the MPC 26-5, MPC 34-1 and MPC 10-4 wells.

	Net to Gross (ft)		
	MPC 26-5	**MPC 34-1**	**MPC 10-4**
Massive Sand	0.99	0.98	0.92
Dantzler	0.95	0.99	1.0
Big Fred	0.94	0.85	0.9
Paluxy Zone 4	0.72	0.75	0.88
Paluxy Zone 3	0.74	0.83	0.7
Paluxy Zone 2	0.9	0.68	1
Paluxy Zone 1	0.87	0.72	0.62

The reservoirs are separated by laterally extensive mudrock seals and are overlain by the Tuscaloosa marine shale, an extensive regional seal. Other, shallower, sealing strata are present in Kemper County, and these include the Porters Creek Clay and Selma Group, which form a regional confining interval that is more than 1,400 feet thick (**Figure 2**) (Pashin et al, 2008). The Porters Creek Clay is a proven seal that holds oil in fractured chalk reservoirs in Alabama and Mississippi and the chalk of the Selma Group forms a regional seal for conventional oil and gas accumulations in the Eutaw Formation (Frascogna, 1957; Davis and Lambert, 1963; Galicki, 1986; Pashin and others, 2000).

2.2 Project ECO$_2$S Data Collection

In 2017, three new geologic characterization/monitoring wells were drilled in the vicinity of Plant Ratcliffe: the MPC 26-5; MPC 34-1 and MPC 10-4 (*Well and Security Installation Report, Deliverable 5.3.a*) and the green box is the area selected for constructing the simulation grid (**Figure 4**).

Data from the three new wells, along with a test well drilled in 2008, informally called the Kemper Water Well, were used to develop the geologic model. The three wells penetrate the potential geologic storage intervals, and their confining zone(s). During the drilling process core was collected from each well to better characterize the subsurface geology by integrating the geophysical log response and petrophysical properties observed in collected core samples (see *Deliverable 6.1 - Core Analysis Report*). The MPC 34-1 and MPC 10-4 cores were selected for sampling for basic core analysis and other petrophysical analysis at a commercial core laboratory. Routine core analysis of selected core samples was used to calibrate the geophysical logs. CT scans and FMI log results from the new wells were used to perform a paleocurrent analysis of the Paluxy (Pashin et al., 2020). From this work, the dominant flow direction was determined to be northwest (Pashin et al., 2020) implying that the higher permeability is in the northwest-southeast direction.

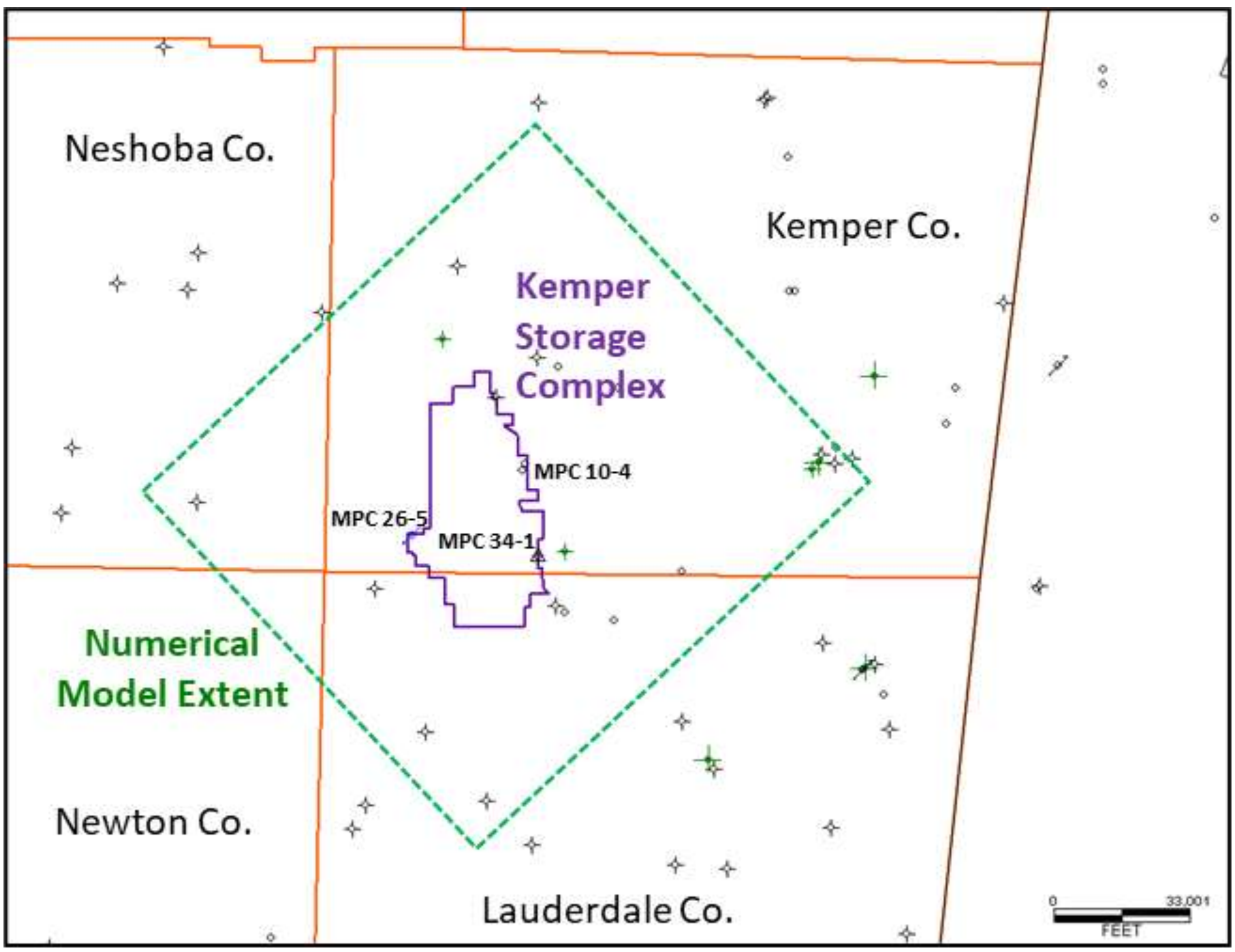

Figure 4: Kemper storage complex, numerical model extent and location of 3 new wells.

2.3 Geologic Model Analytical Approach

The Kemper Regional Storage static geologic model was constructed using the Petra™ (IHS) software. Subsurface maps (structure and isopach) and cross sections of the Cretaceous interval were constructed. Formation tops data were identified, and correlations were extended to the new wells. For the Paluxy and the Washita-Fredericksburg, formation tops were correlated with an attempt to keep the tops at (roughly) the same horizon (flat) because fluvial systems tend to aggrade to the same level (Pashin, pers comm), therefore the top of a sand body is used to correlate from well to well. The surface of the Cretaceous sediments, which contain the target storage reservoirs, are smooth and planar and thicken and deepen to the southwest approximately 70 ft per mile.

The log data was calibrated to the routine core analysis of selected core samples. The porosity average values for the three new wells were then used in the geologic model (**Table 2**). For the Tuscaloosa Massive sand a porosity - permeability cross plot was generated using available Massive Sand routine core analysis data from Jackson county Mississippi (SECARB Phase II Plant Daniel) and porosity and permeability over the Massive sand interval from the MPC 10-4 calibrated petrophysical model (Schlumberger's ELAN probabilistic model). The MPC 10-4 calibrated petrophysical model results were also used to create a porosity- permeability cross plot for the Dantzler. For the Washita-Fredericksburg routine core analysis data from the lower Washita-Fredericksburg (MPC 34-1) and calibrated petrophysical model results from MPC 10-4 were used to generate a cross plot. The Paluxy cross plot was generated from routine core analysis results of core samples from the MPC 10-4 well.

Permeability for all target formations was derived from porosity permeability transforms that were generated from the porosity – permeability cross plots (**Figure 5**). Net reservoir sandstone was estimated using a gamma-ray index cut-off where the gamma-ray index cut-off was determined by calibrating the porosity and permeability from core to the porosity logs. From this, the corresponding gamma ray values were identified and a gamma-ray cut off of 70 API was selected to discriminate between the potential storage flow units (sand) and the inter-burden (shale). After the sandstone intervals were identified the reservoir architecture was defined in the geologic model.

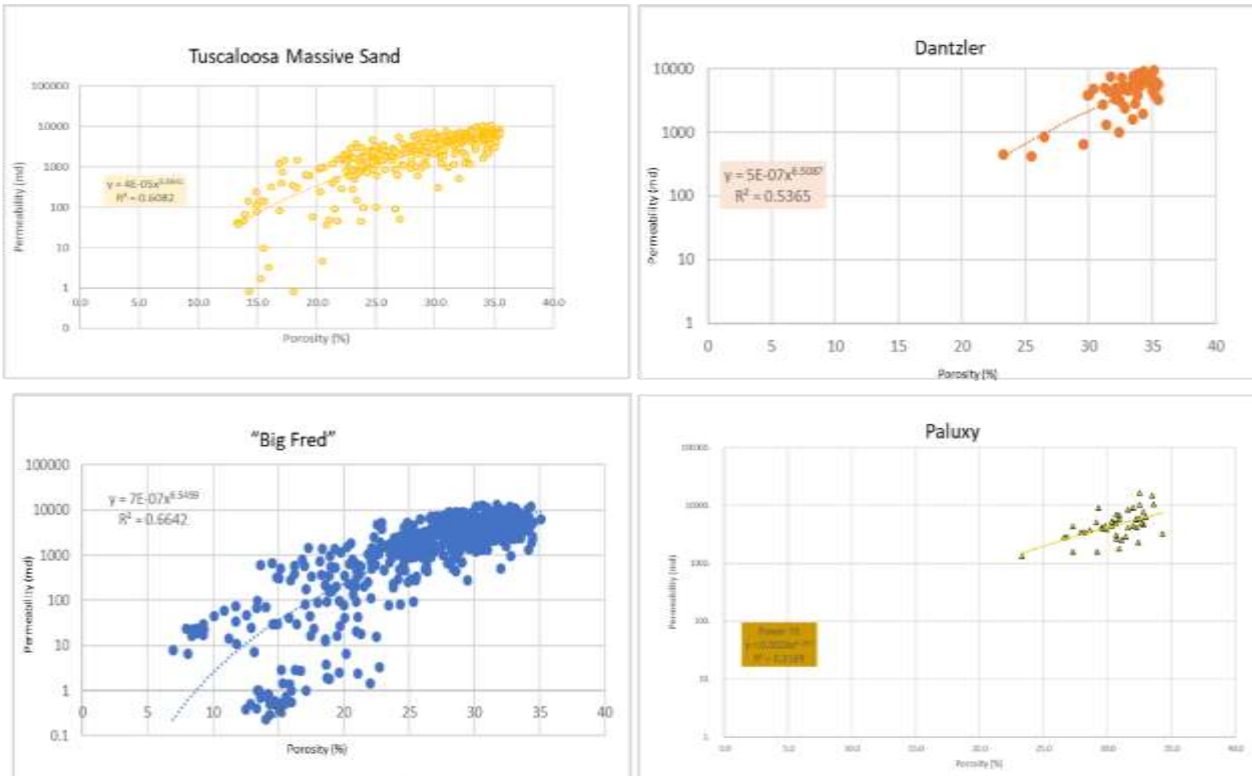

Figure 5: Porosity-Permeability transforms for the target reservoirs.

The sandstone bodies in the Paluxy and Washita-Fredericksburg interval were deposited in a multistory bedload dominated fluvial system (Pashin et al., AAPG 2018). Fluvial sand-bodies are notoriously difficult to correlate even over short distances, and the limited available data complicates the correlation. Due to the difficulty in correlating individual fluvial sand bodies, the Paluxy formation was broken out into 4 major multistory zones, or flow units, that are apparent in the three Phase II wells (the Kemper water well was not drilled into the Paluxy). The 4 zone tops were correlated with an attempt to keep the tops at (roughly) the same horizon (flat). Any shale between the zone tops was included in the overlying zone. This approach was not appropriate for the Big Fred due to the apparent overwhelming influx of sediment that occurred during deposition, which resulted in minimal internal shale breaks. As such, the Big Fred was not broken out into multiple zones in the geologic model, but instead is treated as a single flow interval. The

Dantzler and the Massive Sand are also predominately sand and were not separated as multiple flow units, but instead each was correlated as a single flow unit.

Once the flow units were correlated, a net to gross ratio for each flow unit from each of the 3 new wells was determined using the gamma ray cutoff and the average of the three was assigned to each flow unit**. Figure 6** shows a structural cross section of the three storage reservoirs and **Figure 7** shows the 4 zones that were delineated in the Paluxy along with the total net to gross for the Paluxy in each well. Studies have shown that the net-gross ratio can provide information on how disconnected a fluvial sequence is (Allen, 1978) and that high net-gross sand ratios indicate a high degree of connectivity (King, 1990; Allard and HEREISM Group 1993). For example, work by Allen (1978) on 2-D models showed that in fluvial successions with 50% or less overbank mudstones, virtually all sandstone bodies are disconnected. However, once proportion goes above 50%, the degree of connectivity rises steeply. King (1990) and Allard and HEREISM Group (1993) documented that connectivity remains low until a certain sand percentage is reached; this is the percolation threshold. The percolation threshold in 2-D models occurred at about 60% net to gross and 25% net to gross in 3-D models. The net to gross for each of the potential storage reservoirs is given in Table 2. All three potential storage reservoirs have high net to gross ratios suggesting a high degree of connectivity and communication.

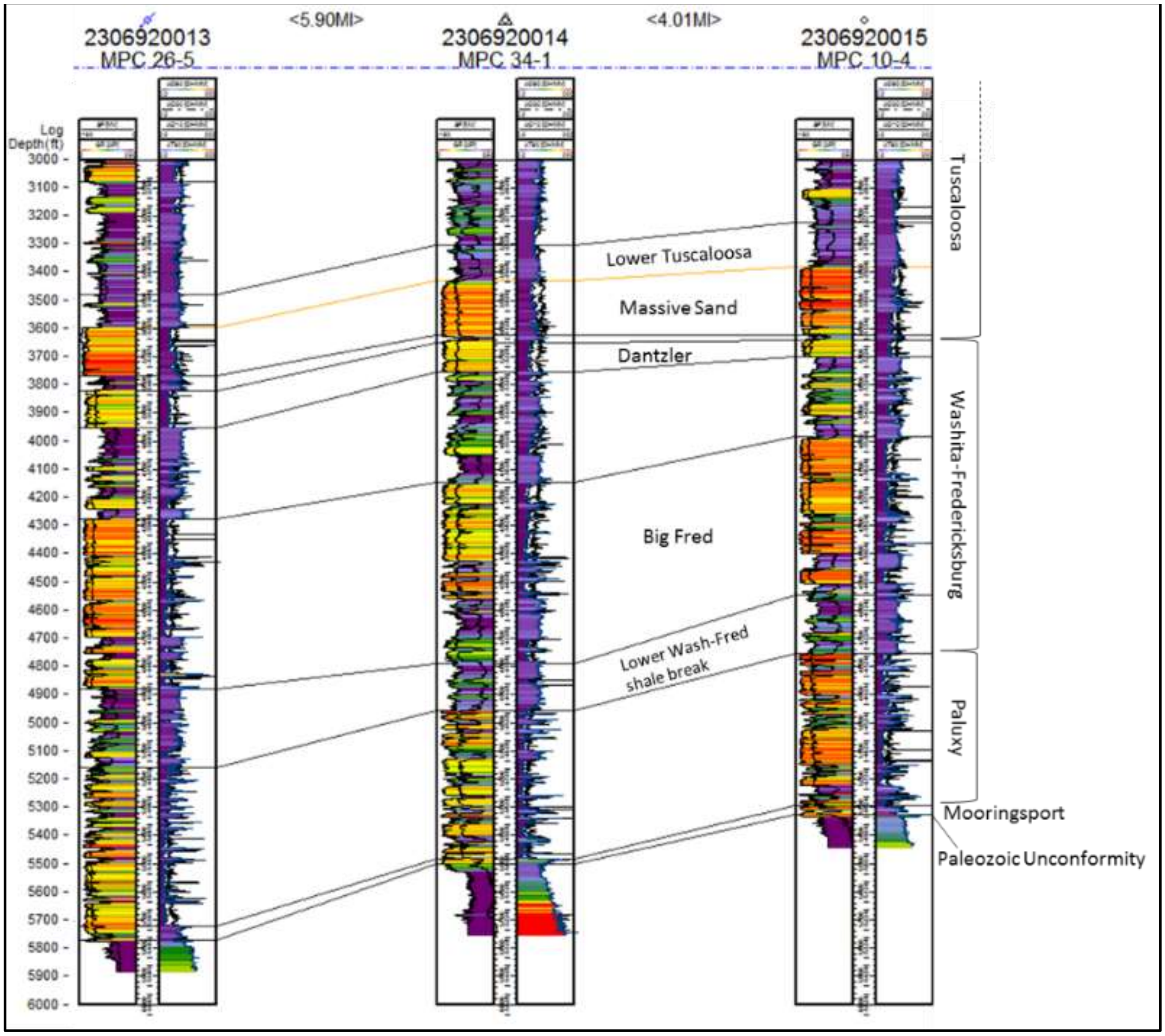

Figure 6: Structural cross section between the three Project ECO$_2$S wells.

The left-hand track shows natural gamma ray and spontaneous potential curves. The gamma ray curve is geo-shaded where warmer colors indicate lower gamma ray and, likely, cleaner sands. Cooler colors indicate higher natural gamma ray and increasing shale content. The right-hand track shows resistivity curves.

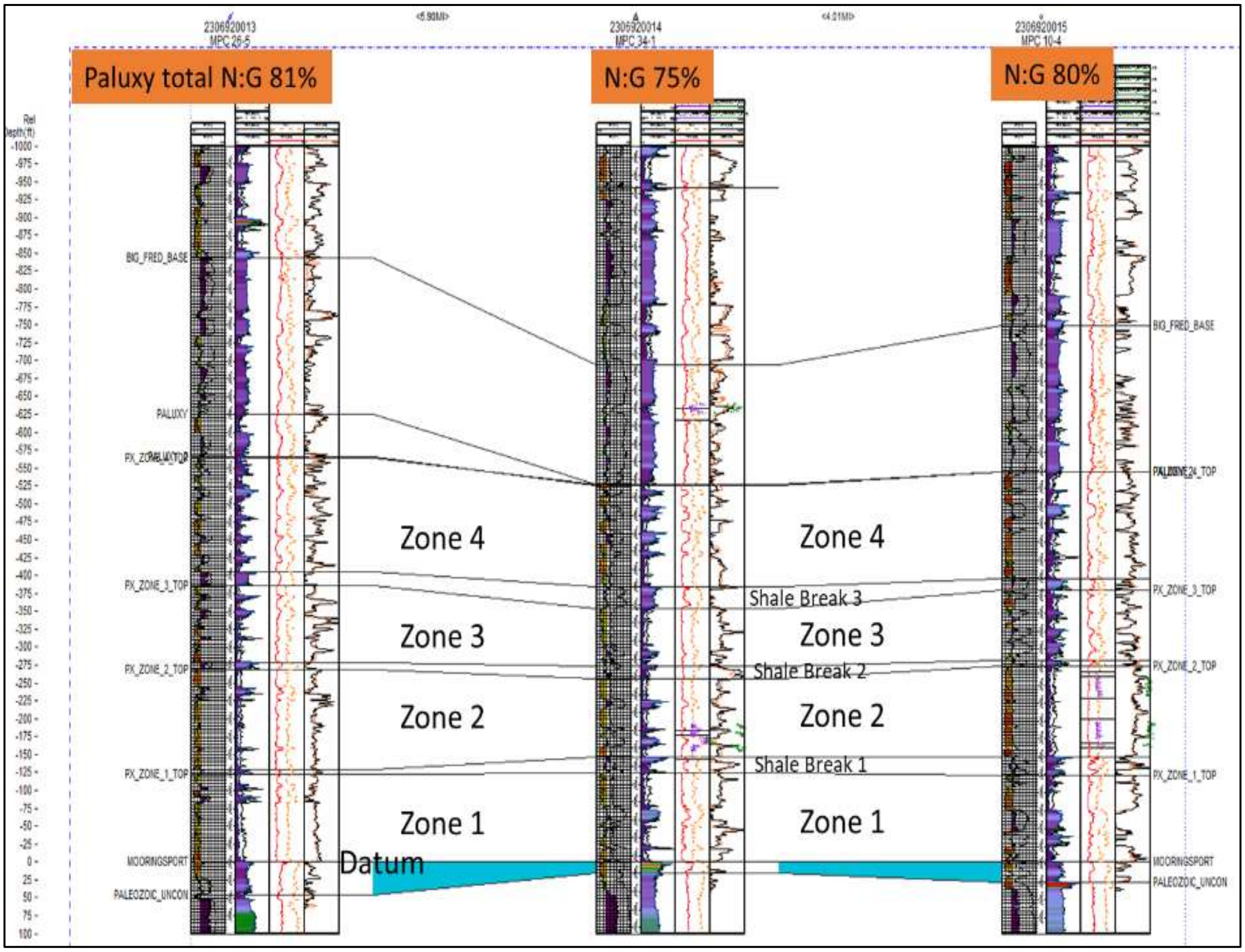

Figure 7: Stratigraphic cross section showing the Paluxy defined zones for the new 2017 Kemper Project ECO$_2$S wells (MPC 26-5, 34-1, and 10-4).

The cross section is hung on the Mooringsport formation.

Average rock properties of the layers, including the three target formation groups, are summarized in **Table 3**. The target reservoirs are highlighted.

Table 3: Average reservoir properties in the base simulation model. Target formations are highlighted

Reservoir Name	Thickness, ft	Net Pay, ft	Porosity, frac	Geometric average of horizontal permeability (mD)	K_vert/K_hor
Upper Tuscaloosa	500	500	0.1	5.0E-04	1
Marine Tuscaloosa	348	348	0.1	5.0E-04	1
Lower Tuscaloosa	114	114	0.1	5.0E-04	1
Massive Sand	220	211.2	0.3	3,353	1:10
Dantzler	105	102.9	0.33	4,083	1:10
Upper Wash-Fred	348	348	0.1	5.0E-04	1
Big Fred	430	387	0.27	1,269	1:10
Lower Wash-Fred	376	376	0.1	5.0E-04	1
Paluxy Zone 4	178	138.84	0.25	708	1:10
Paluxy Zone 3	104	79.04	0.27	1,079	1:10
Paluxy Zone 2	160	137.6	0.28	1,486	1:10
Paluxy Zone 1	120	88.8	0.25	708	1:10
Mooringsport	32	32	0.1	5.0E-04	1

A horizontal permeability anisotropy of 3:1, with the higher permeability in the northwest-southeast direction, and on structural strike, was employed in the model. This ratio was obtained from a simulation model calibrated to an analog reservoir at the Anthropogenic Test Site at Citronelle, Alabama (Advanced Resources International, 2016) and the anisotropy direction was obtained from the paleocurrent analysis (discussed previously). During phase III of this project, special attention will be given to evaluating the horizontal permeability anisotropy ratio and the direction of the higher permeability. Additional observation wells around the storage site would provide valuable information on CO_2 movement and better estimating the permeability anisotropy through reservoir simulation and history matching. At this time, well drilling and geologic data at the site is insufficient to adequately assess this parameter. Additional well drilling and acquisition of 3D seismic volume during Phase III will focus on addressing this uncertainty. Due to the fluvial nature of these formations, the vertical permeability is assumed to be lower than the horizontal permeability. A ratio of 10:1 was used to generate vertical permeability from the geometric average of the horizontal permeability. This ratio was estimated from the Citronelle Paluxy formation interpretation. Due to lack of data for the remaining reservoirs, the same ratio was applied to all the reservoirs in the model.

3.0 Numerical Modeling

3.1 Modeling Software

Computer Modeling Group's (CMG) *GEM* reservoir flow simulator is employed to model the subsurface injection of CO_2 into the target formations at the Kemper storage complex. *GEM* is an industry-standard, Equation-of-State, fully compositional, three-dimensional reservoir simulator for modeling the flow of three-phase, multi-component fluids. In addition to modeling CO_2 injection, *GEM* has the capability to model several CO_2 trapping mechanisms, such as residual gas trapping via relative permeability hysteresis, CO_2 dissolution into the aqueous phase and intra-aqueous reactions, as well as mineral trapping and precipitation. Among these mechanisms, only the hysteresis and dissolution trapping are modeled in this study.

3.2 Grid Construction

The numerical model uses a corner-point grid with 136 grid cells in the x-direction and 262 grid cells in the y-direction. The grid is rotated 300 degrees to align the x-direction to the high permeability direction. Individual grid blocks are 850 feet in x-direction by 500 feet in the y-direction, with the appropriate depth and thickness values. The total areal dimension of the grid is 115,600 feet by 131,000 feet, or 543 square miles. Each target reservoir was subdivided into multiple layers to get an average cell thickness of about 20 feet. **Figure 8** shows a 3D view of the grid.

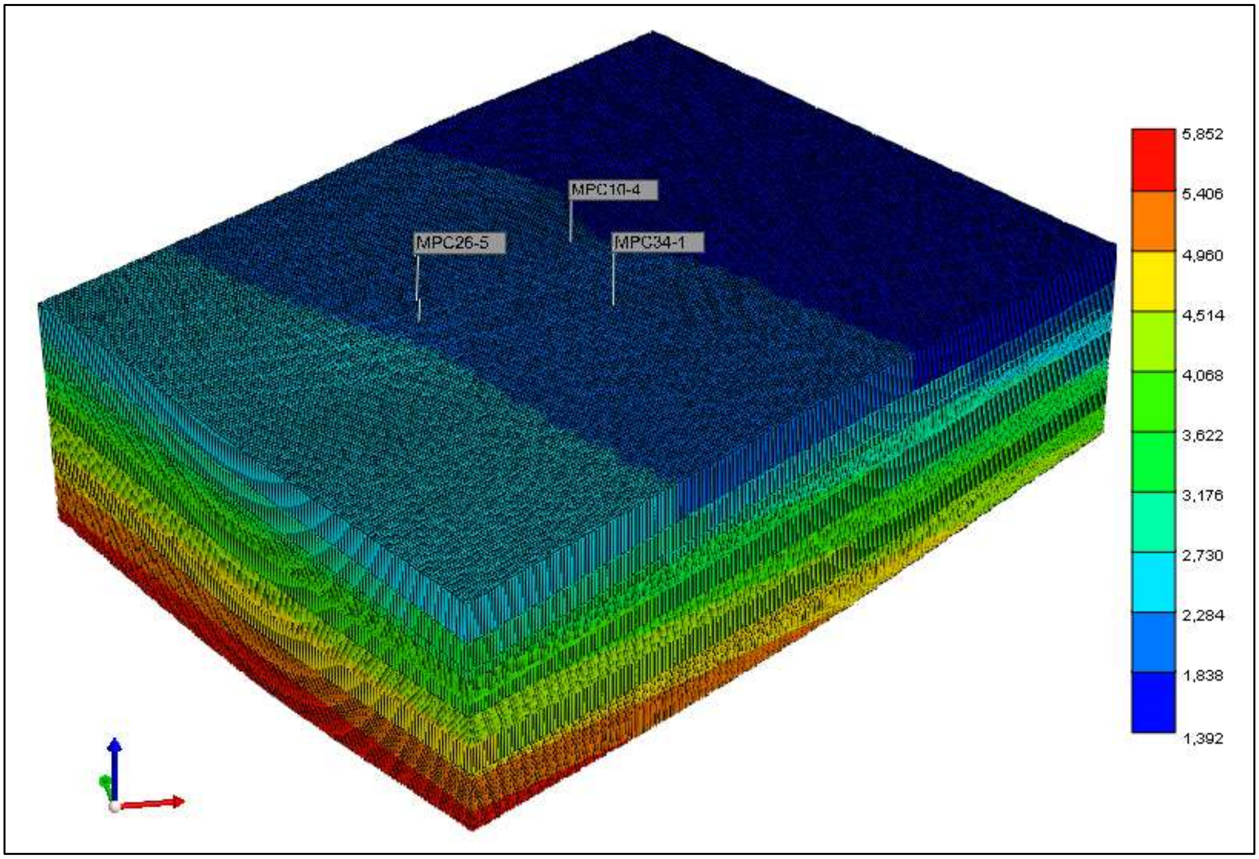

Figure 8: Kemper model grid elevation (TVDSS in feet)

A larger area beyond the injection site was included in the model to simulate the interaction of a larger saline reservoir with the injected CO_2.

Figure 9 shows the simulation grid. The grid is rotated by 300 degrees to align the cells in I direction to the high horizontal permeability direction.

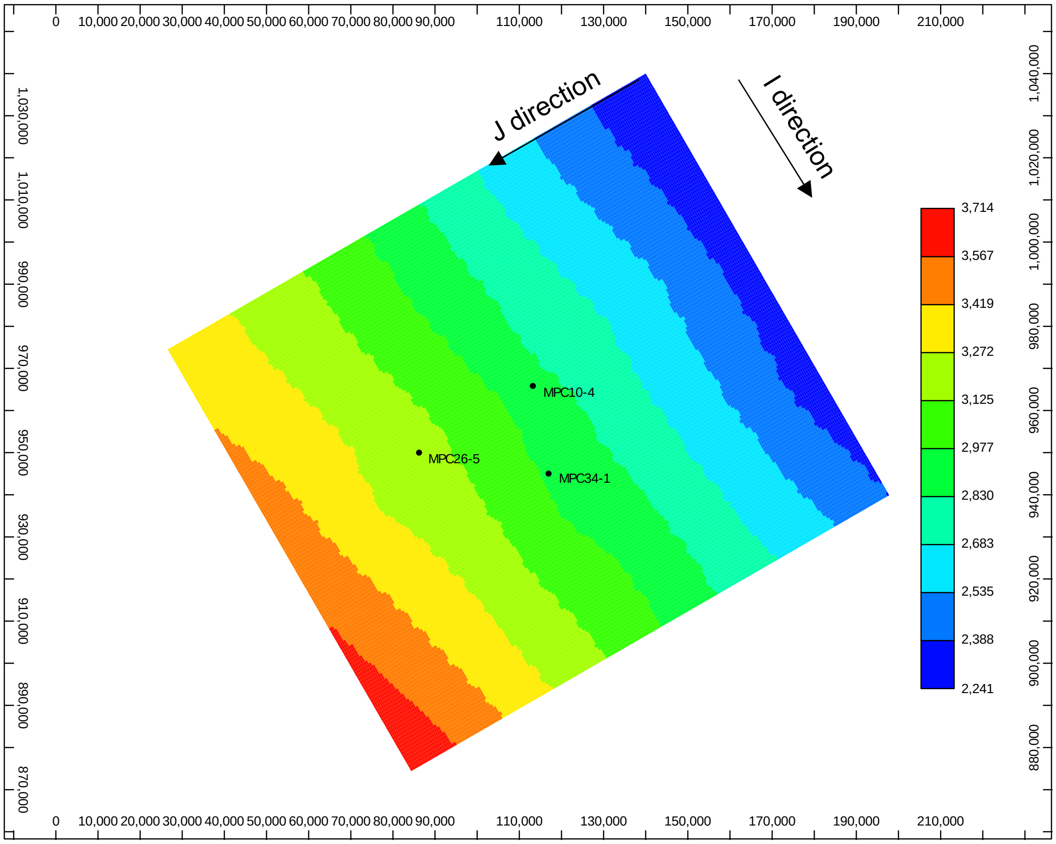

Figure 9: Kemper model grid, showing the elevation (TVDSS in feet) of the Massive Sand.

3.3 Fluid and Pressure Properties

The model was initialized with three regions to properly account for variable reservoir pressures and salinity values in each target reservoir group. These values were obtained from water sample analysis (Advanced Resources International, 2020) and well test interpretation (Jalali, 2019). Initial reservoir pressures and their corresponding reference depth and salinity values are provided in **Table 4**.

Table 4: Kemper model initial reservoir pressure, temperature, and salinity value for each region

Target Reservoir	Reservoir Pressure (psia)	Reference Depth (feet)	Salinity, mg/l	Temperature, F
Massive/Dantzler	986	3,150	23,000	112
Wash-Fred	1,363	3,720	85,271	125
Paluxy	1,813	4,482	115,531	129

The simulation model is initialized as a two-phase gas-water system. Two-component Equation of State is constructed with CO_2 as the non-hydrocarbon component and C_1 as the hydrocarbon component. **Table 5** shows the properties of these two components that are used in the simulator for EoS calculations. Since all the reservoirs are saline formations, the model is initialized with 100% brine.

Table 5: Component properties for the Equation of State

Property	CO_2	C_1
Critical pressure, atm	72.8	45.4
Critical temperature, K	304.2	190.6
Acentric factor	0.225	0.008
Molecular weight, g/gmole	44.01	16.043
Critical volume, m^3/kgmole	0.094	0.099
Specific gravity (SG)	0.818	0.3
Average normal boiling point (Tb), F	-109.21	-258.6
Parachor	78	77

3.4 Rock-Fluid Properties

The relative permeability data used for this study were borrowed from work conducted in the Paluxy formation at the Anthropogenic Test Site at Citronelle, Alabama (Advanced Resources International, 2015). These curves were generated through history matching the CO_2 injection history pressure and CO_2 breakthrough response monitored at multiple offset well locations. **Figure 10** shows the relative permeability curves used in this model.

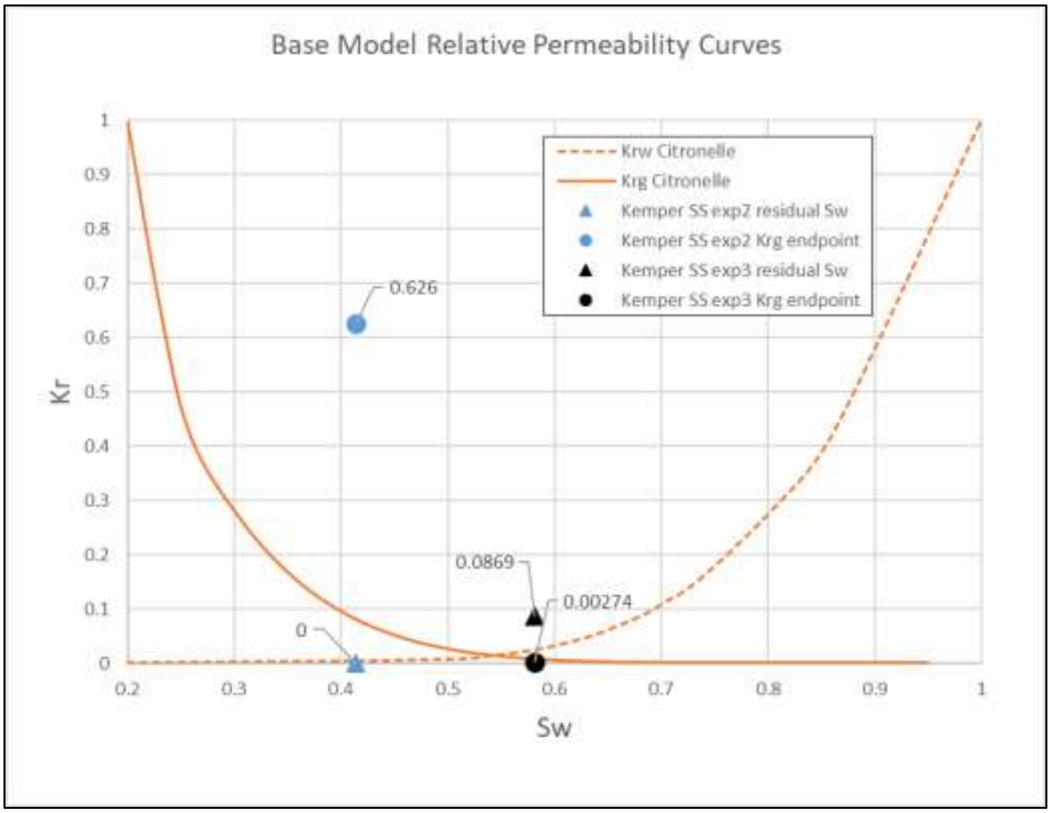

Figure 10: Relative Permeability Curves used in the Kemper model.

Additionally, the endpoints from two steady-state relative permeability tests that were performed on two Paluxy core samples within the Kemper site area (Akbarabadi, Arshadi, & Khishvand, 2019) are added to **Figure 10**. However, the relative permeability curves from the test were not used in the simulation model. The reason for this is the general concern with the CO_2-brine relative permeability test interpretations, which is the implicit assumption that the brine is the wetting phase and the supercritical or the liquid

CO_2 is the non-wetting phase. We know that CO_2 and brine are mutually soluble. Due to solubility of CO_2 in the brine, some transfer of CO_2 can occur through the water film lining pore walls and adhere to the underlying solid surface. As a result, the wettability of the pore system might be altered in some instances. The dissolution of CO_2 into brine and possible adsorption of CO_2 on mineral surfaces can reduce the displacement of brine by the injected CO_2 resulting in a higher residual brine saturation and reduction in endpoint CO_2 saturation (Levine, 2011) (Berg, Oedai, & Ott, 2011).

CO_2 trapping due to hysteresis is another mechanism that was modeled here. When CO_2 injection starts, the CO_2 is immobile until it reaches a critical gas saturation. Once the CO_2 saturation exceed its critical saturation, it will be able to move through the pore system. When CO_2 saturation is reduced in a pore volume due to brine influx, it will become immobile at a saturation that is higher than the original critical saturation. The new trapping saturation can have a value between the critical gas saturation and one minus the irreducible water saturation. The hysteresis option was activated within the model to simulate hysteresis trapping. A maximum residual gas saturation of 15% was chosen as a conservative value for the hysteresis curve in the base model.

3.5 Injection Site Conceptual Design

At the injection site, a total of seven CO_2 injection pads were considered in the simulation model positioned in two rows at a northwest-southeast orientation. This number of injection pads was selected to safely inject the required 22.5 MM metric tons of CO_2 volume per year. The first row consisted of two injection pads followed by five pads placed on the second row, down-dip of the first row. Each injection pad was placed 2 miles from the neighboring pad. Three CO_2 injection wells are put on each pad, with each well responsible to inject CO_2 into a specific target reservoir group. This way, different injection rates can be assigned to each target reservoir. Since the Massive Sand and Dantzler have relatively lower thickness than Big Fred and Paluxy and are in close proximity to each other (as shown in the cross section Figure 6), they are grouped together and receive CO_2 from the same injection well. This design will result in drilling a total of 21 CO_2 injection wells.

The center of the storage site was selected to place the CO_2 injection pads in the simulation model. **Figure 11** shows these potential CO_2 injection sites relative to the three Phase II MPC wells.

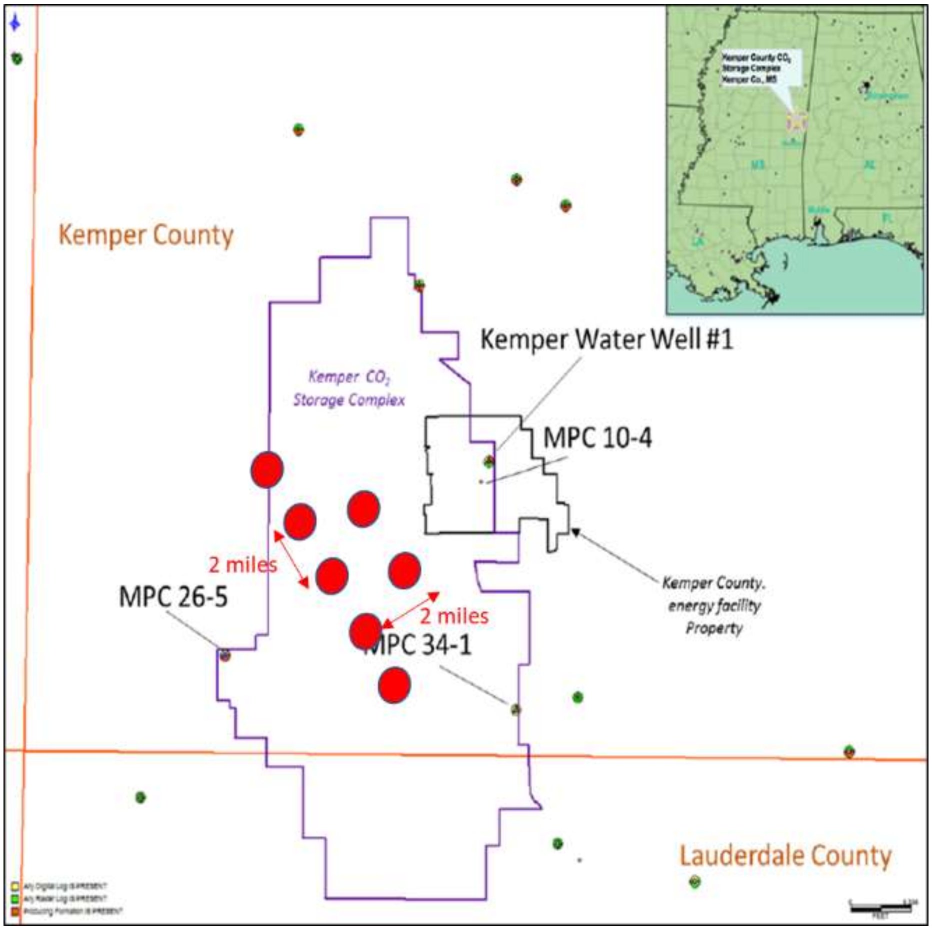

Figure 11: Kemper base model CO_2 potential injection sites

A total of 675 million metric tons of CO_2 was injected into the three target reservoirs over 30 years, at an equivalent injection rate of about 1.2 Bscf per day. The CO_2 plume covered approximately 55 square miles at the top of the Massive Sand formation (**Figure 13**). At the onset of this work, the CO_2 stream was subdivided into three equal injection streams. However, the CO_2 plume in the Massive Sand, expanded to a larger area, resulting in an unbalanced plume size as compared to those in the Big Fred and Paluxy. Therefore, injection rates were modified to generate roughly the same plume sizes in these reservoirs.

To create a similar CO_2 plume areal extent in all three reservoirs, different injection rates were assumed for each reservoir group based on reservoir permeability and thickness. It was observed that similar plume sizes in all three reservoirs could be achieved by injecting 50% of the volume into the Paluxy, 30% into the Big-Fred, and the remaining 20% into the Massive Sand/Dantzler.

All the CO_2 injection wells are perforated through the entire interval of the target reservoir groups. The primary well constraint for these wells is set to be the CO_2 injection rate. A maximum bottom-hole pressure was applied to the CO_2 injection wells as the secondary well constraint to avoid fracturing the rock. The assigned well injection rates and maximum BHP values are provided in **Table 6**.

Table 6: Injection Rate and Max. Well BHP for Target Reservoirs

Target Reservoir	Injection Rate, MMscf/d	Max. BHP, psi
Massive Sand/Dantzler	33.9	2,300
Wash-Fred	50.9	2,600
Paluxy	84.8	3,800

CO_2 hysteresis trapping and brine-dissolution trapping are modeled. Maximum residual gas saturation due to hysteresis is assumed to be 15%. Harvey's correlation was employed in the simulation model to calculate CO_2 Henry's constant to track its solubility in the brine.

3.6 Water Cycling Model

As a part of the sensitivity analysis to study the impact of different parameters on plume areal extent and migration, water cycling was conducted during and post CO_2 injection. In all the water cycling scenarios, water cycling started at the same time as the CO_2 injection and continued 30 years after the end of CO_2 injection. A total of 240,000 STB/D of water was extracted from 12 water production wells (4 for each target reservoir group at a rate of 20,000 STB/D/well) from parts or the entire interval of the reservoir and injected back into the reservoirs through 12 water injection wells. The water production wells were placed on 4 pads, with each pad hosting three wells producing from each target formation (Massive/Dantzler, Big Fred, and Paluxy). A similar setup was employed for the water injection wells. Sensitivity analysis was performed on the perforation interval and placement of water injection and production wells. Depending on the sensitivity case, the water production and injection wells were either perforated in the entire target formation interval or partially perforated.

3.7 Sensitivity Analysis

The parameters and their values used in the sensitivity analysis are provided in **Table 7**.

Table 7: Kemper model sensitivity parameters

Parameter	Sensitivity Values	Base Value
Horizontal Permeability Anisotropy	1:1, 3:1	3:1
Water cycling wells location	3 scenarios	-
Water Injector Perforation Interval	Top 100 feet, Entire Interval	-
Hysteresis maximum residual gas saturation	5%, 15%, 40%	15%

In the next section, the results of these models are presented.

4.0 Results and Discussion

This section presents the results of the base case, followed by the results of the sensitivity analysis on water cycling scenarios and other reservoir parameters.

4.1 Base Model (Case 1) Results

Figure 12 shows the injection rate and flowing bottom-hole pressure of the injection wells for the three target reservoir groups. During the 30-year injection period, the flowing bottom-hole pressure did not reach the maximum allowable pressures and the entire planned CO_2 injection volume was placed in the reservoir. There is an initial increase in the wells' bottom-hole pressure at the start of CO_2 injection. This may be because CO_2 has not reached its critical saturation within the well block (no local grid refinement used around wells) and it is still immobile. Once the saturation exceeds the critical value of 5%, it can move outside the well blocks and pressure decreases. At the end of injection, the bottom-hole pressures stay elevated and do not return to near initial reservoir pressure. This is because we are simulating a closed system.

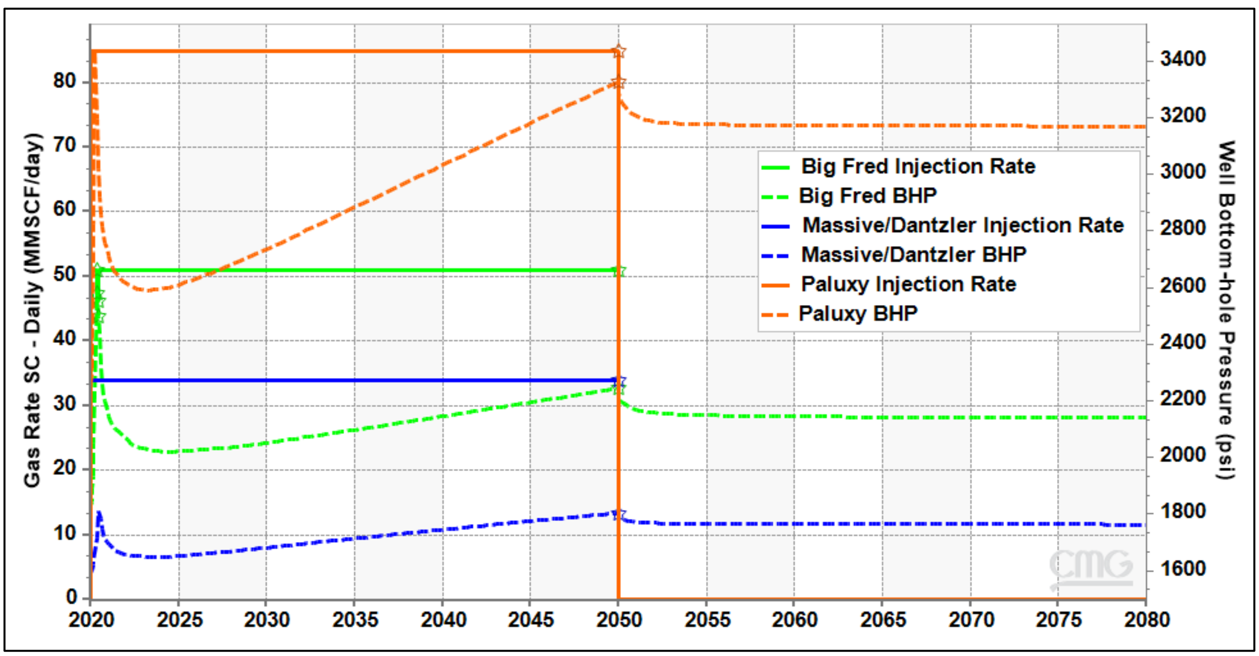

Figure 12: Kemper base model CO_2 injection rates

Figure 13 shows the largest CO_2 plume, which is formed at the top of the Massive Sand formation (gas saturation greater than 5%), in the base model through different times.

During the CO_2 injection period, the plume grows in all directions. However, after the end of injection, the CO_2 plume tends to get wider and migrates up-dip.

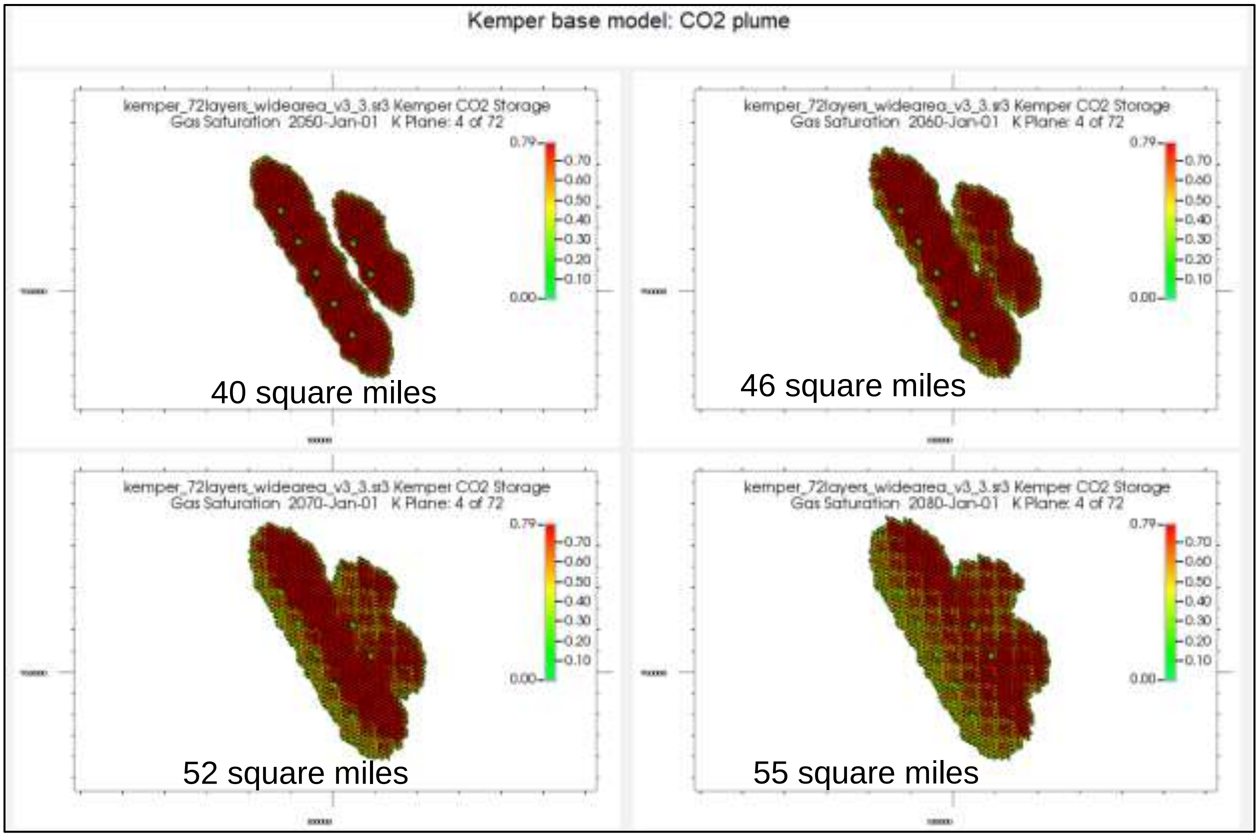

Figure 13: Kemper base model CO_2 plume at the top of Massive Sand. Top-left: and the end of injection, top-right: 10 years post injection, bottom-left: 20 years post injection, bottom-right: 30 years post injection

Figure 14 shows the estimated plume size for each target reservoir group at different times after the end of CO_2 injection.

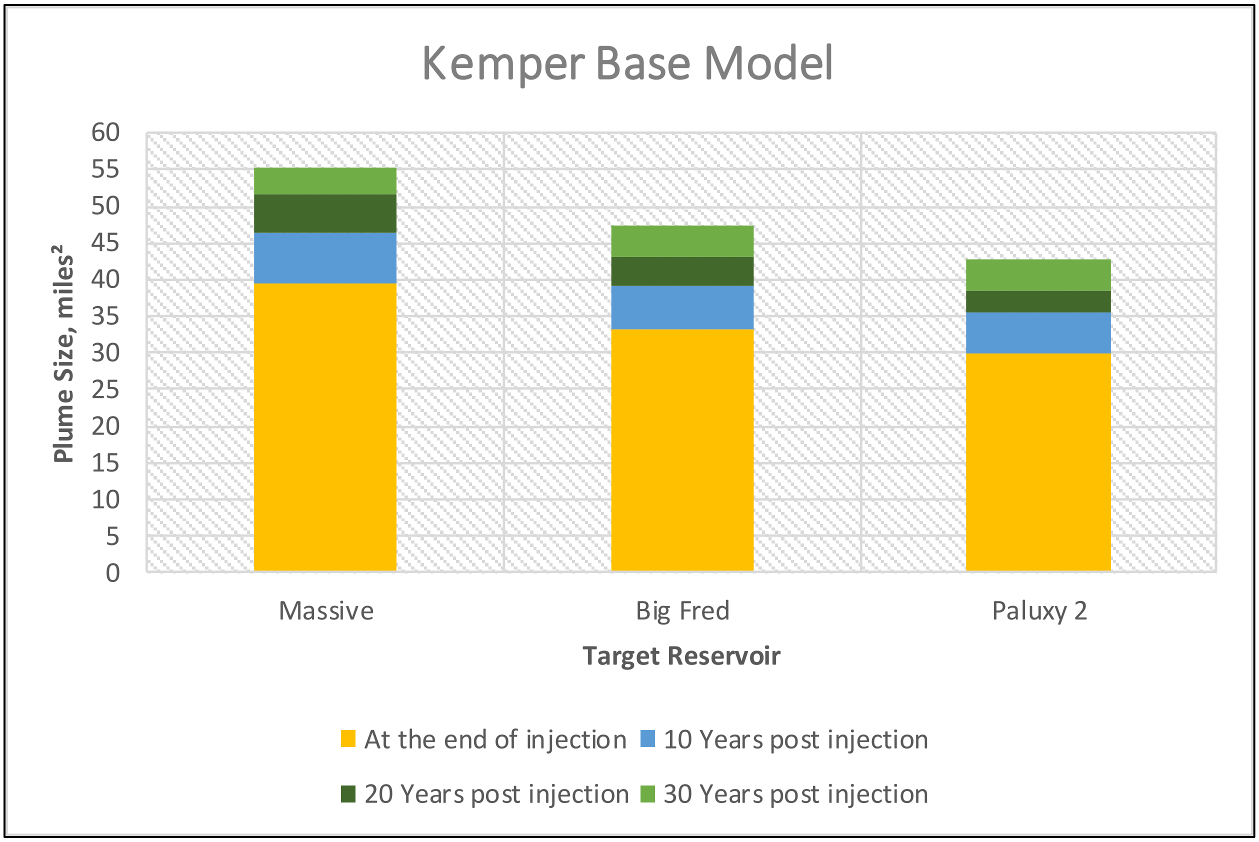

Figure 14: Base model plume sizes in the three target reservoir groups

The largest plume is developed at the top of the Massive Sand reservoir, which is the shallowest of the three target formations. The reason for a larger plume size in this reservoir might be due to the lower density of the super-critical CO_2 (shallower depth) resulting in larger buoyancy effect when compared to the deeper formations. As a result, most of the CO_2 migrates to the top of the formation and then moves laterally under the cap rock. **Figure 15** shows the CO_2 mass density in the three reservoirs, ranging from 38.4 lb/cu-ft at the top of Massive Sand to 48 lb/cu-ft in the Paluxy formation.

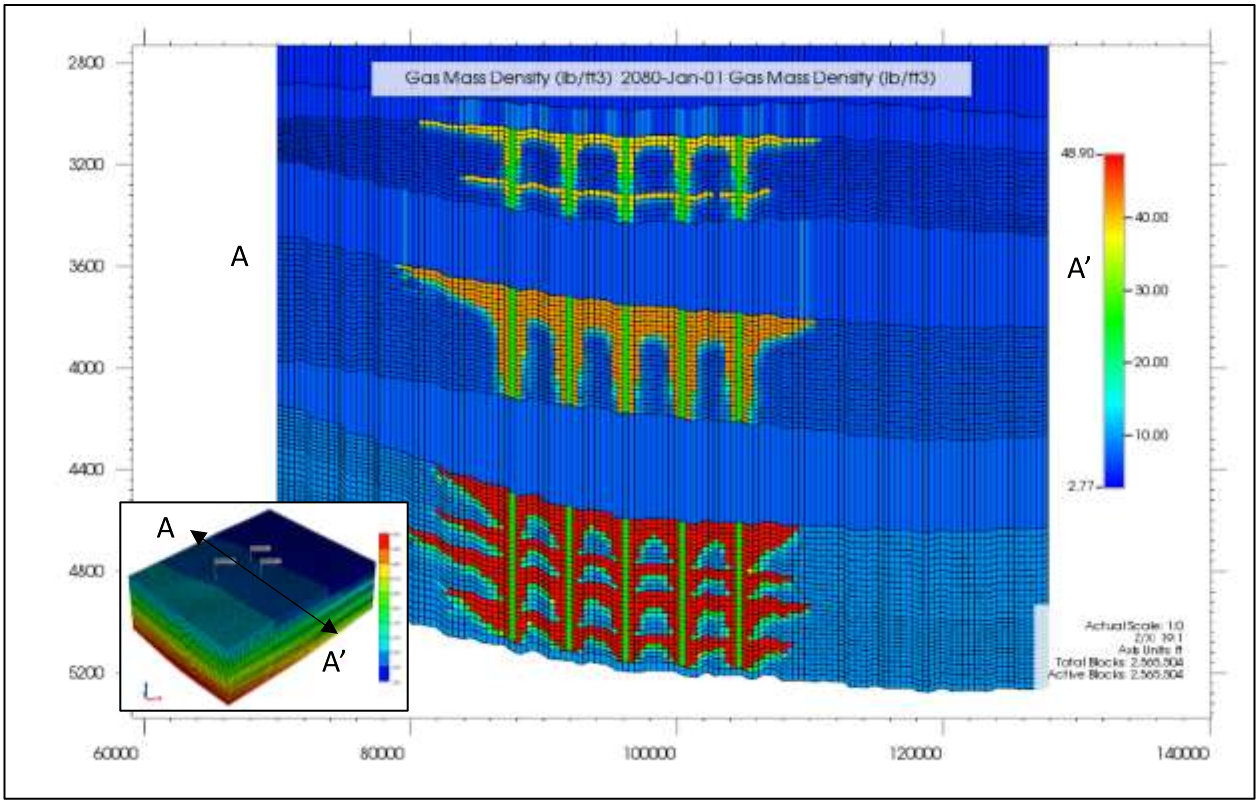

Figure 15: Base model cross section showing CO_2 density, 30 years after the end of injection

CO_2 solubility in brine (**Figure 16**) is mostly less than 2% and is similar in all three reservoirs.

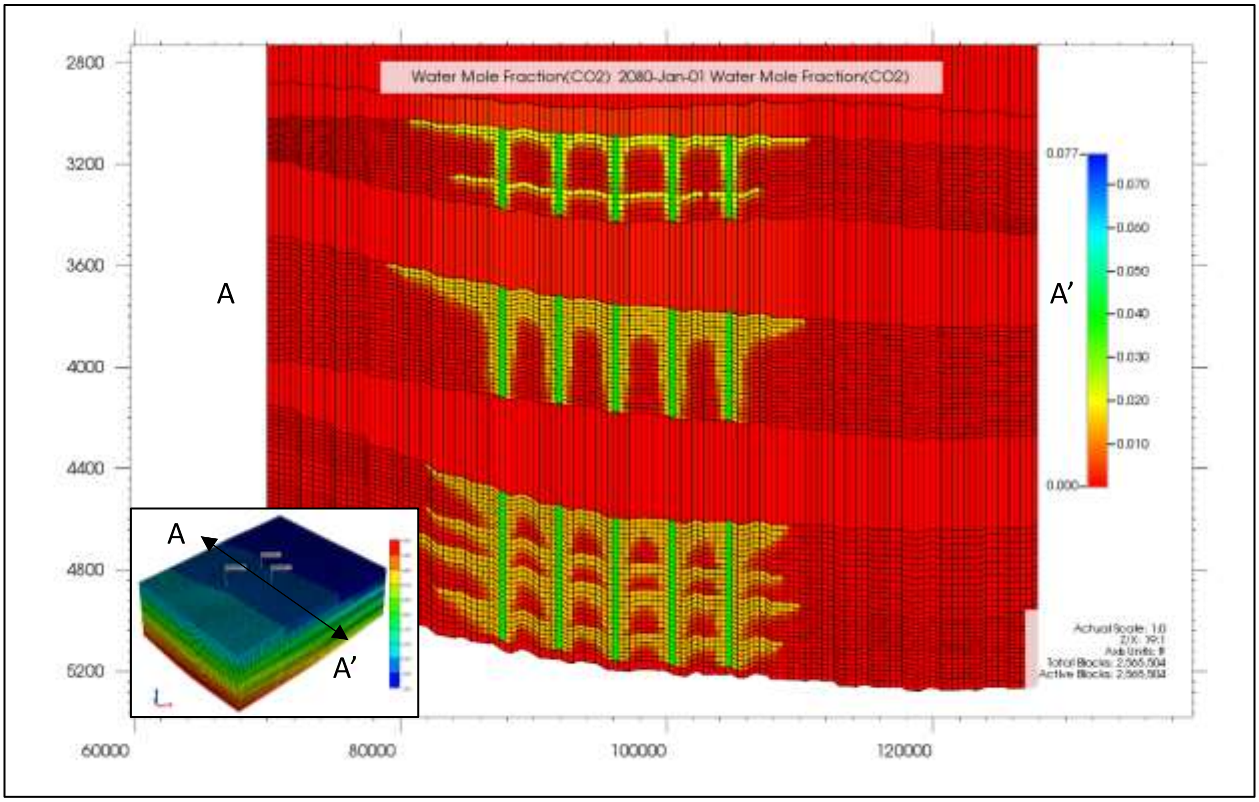

Figure 16: Kemper base model cross section showing CO_2 solubility in brine, 30 years after the end of injection

Figure 17 shows the dynamic trapped gas saturation in the model 30 years after the end of CO_2 injection. The figure is a cross-section of the model along the large plume and in the direction of the higher horizonal permeability. As it can be seen in this map, the top of the target formations still show that the higher 15% residual gas saturation has not yet been activated. This means that the CO_2 saturation at the top layer is still increasing due to migration of the CO_2 from the lower layers.

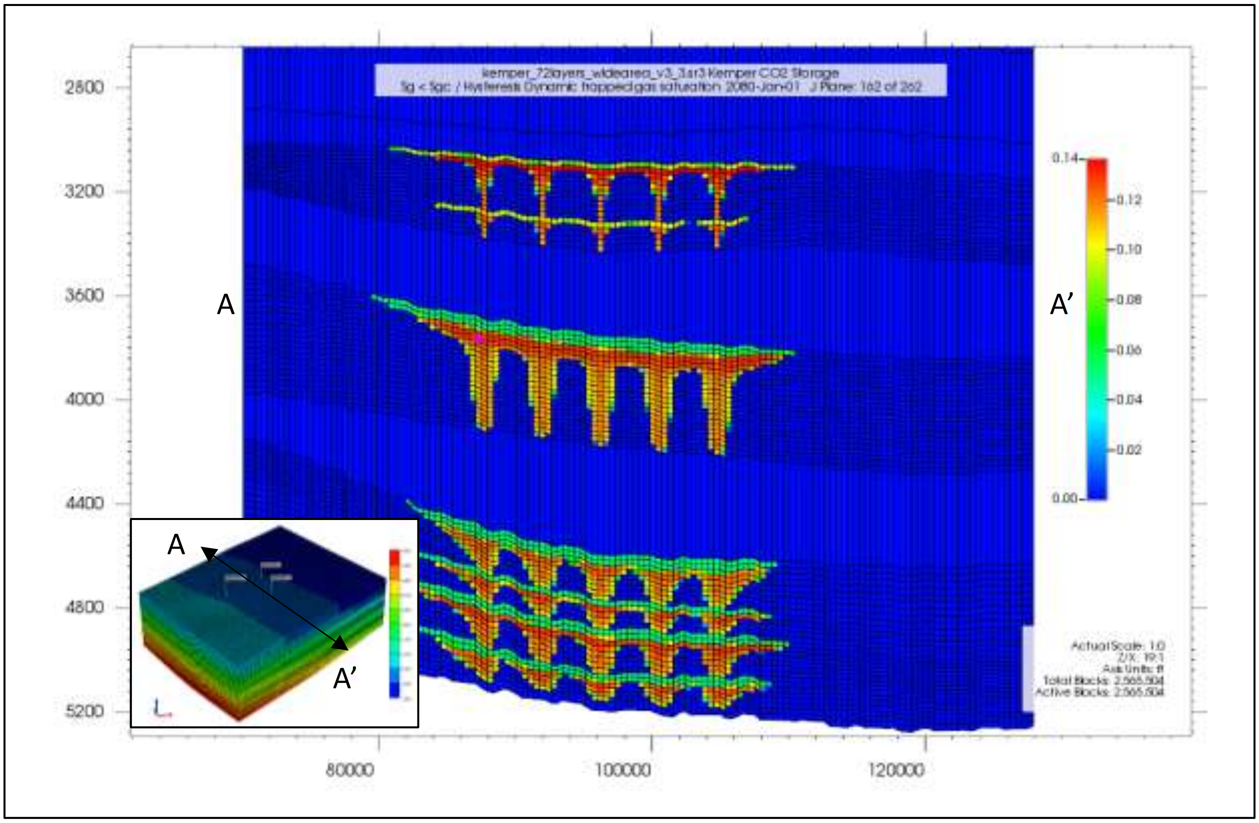

Figure 17: Kemper base model cross section showing the dynamic trapped gas saturation, 30 years after the end of injection

5.0 Sensitivity Analysis

In this section, sensitivity analysis on horizontal permeability anisotropy, water-cycling configuration, and hysteresis trapping gas saturation (Sgrmax) is presented.

5.1 Sensitivity Analysis – Horizontal Permeability Anisotropy (Sensitivity 1)

As discussed earlier, the horizontal permeability anisotropy assumption of 3:1 is borrowed from the calibrated Citronelle model. A model with no horizontal permeability anisotropy was constructed and the plume size generated from this model was compared with the 3:1 anisotropy case. **Figure 18** shows the plume size of the two models at the top of the Massive Sand -30 years after the end of CO_2 injection. In the case of no horizontal permeability anisotropy, the CO_2 plume will cover an area of approximately 70 square miles, compared to 55 square miles in the base case, a 27% difference.

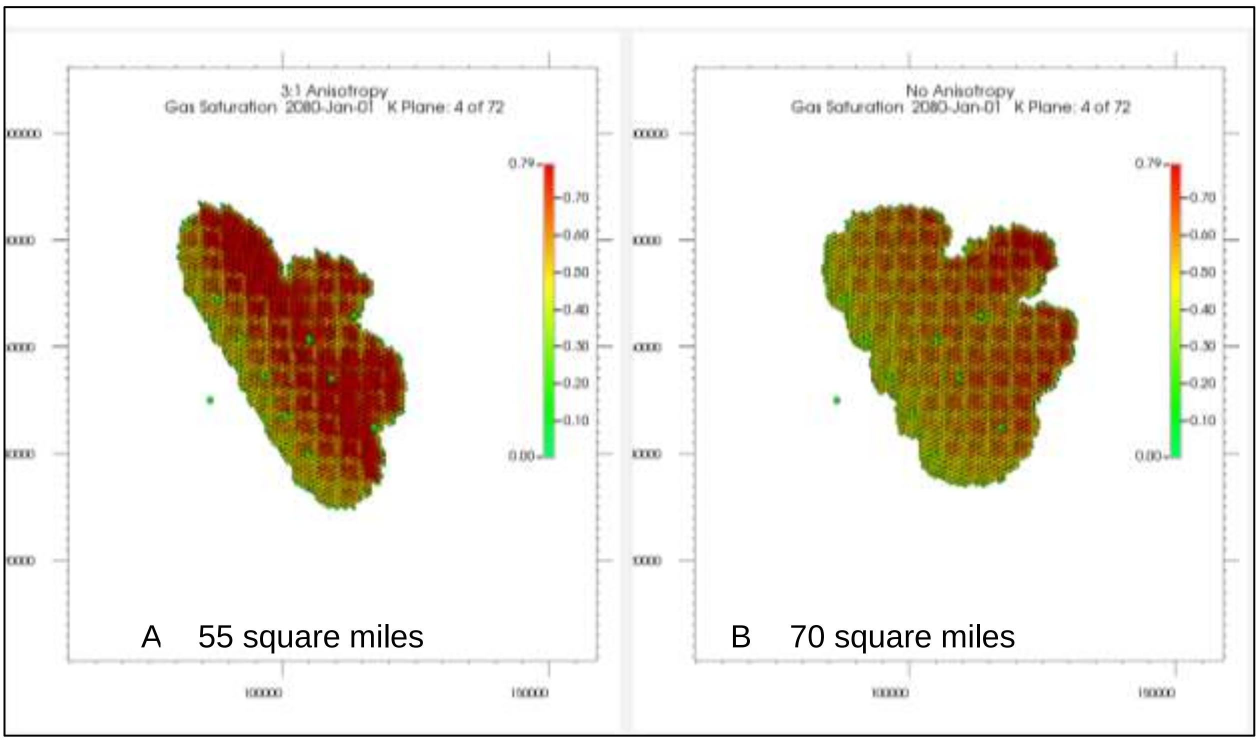

Figure 18: Kemper model permeability anisotropy sensitivity analysis. A) 3:1 anisotropy B) no anisotropy

Active plume management in the form of water cycling was tested to study its impact on the CO_2 plume size and migration. Next, the results of different water cycling scenarios are presented and discussed. The sensitivity study included changing the location of water injection and extraction wells, and the perforation interval in the water injection wells. The impact of these parameters on the CO_2 plume size is presented for each case. Also, the hysteresis trapping gas saturation (Sgrmax) value was changed in the full-interval perforation water-cycling scenario to study the impact of this hysteresis parameter on the plume size.

5.2 Sensitivity Analysis – Water Cycling Well Location (Sensitivity 2)

Different water cycling well configurations were tested to examine their effect on the CO_2 plume extent. Three different scenarios were generated, and their results are presented next.

A water cycling case (Sensitivity 2a) was constructed by placing the four water extraction pads on the Southwestern part of the CO_2 injection site (down-dip of the CO_2 injectors), and the four water injection pads on the Northeastern part of the CO_2 injection site (up-dip of the CO_2 injectors), as it is shown on **Figure 19**.

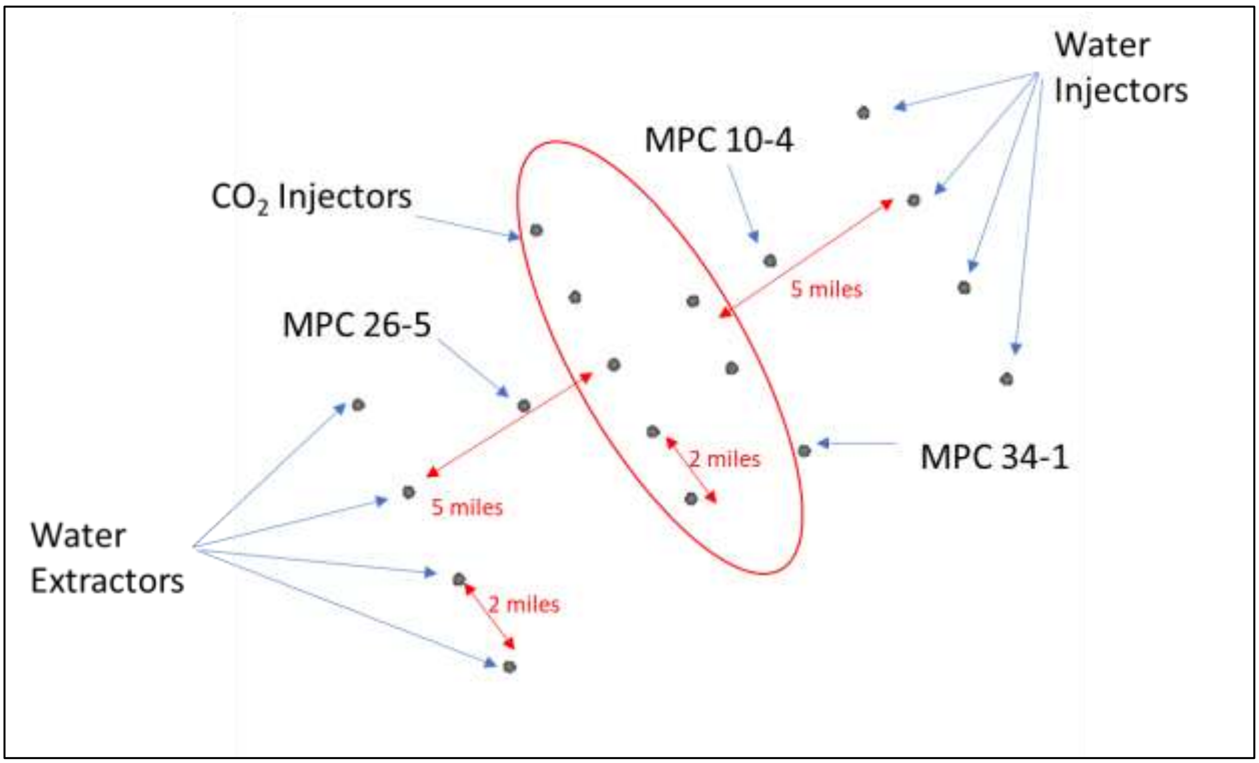

Figure 19: A water cycling scenario (Sensitivity 2a) - well location map

Both sets of water injection and extraction wells were perforated through the entire target reservoir intervals. A 60-year water cycling scenario (30 years during CO_2 injection and 30 years of post CO_2 injection) was run and the CO_2 plume size and movement was evaluated and compared with the base model. **Figure 20** shows the impact of this water cycling scenario on the plume size in all three reservoirs. The plume size in the Big Fred and Paluxy formations are essentially the same in both cases. The meaningful impact is seen in the Massive Sand formation.

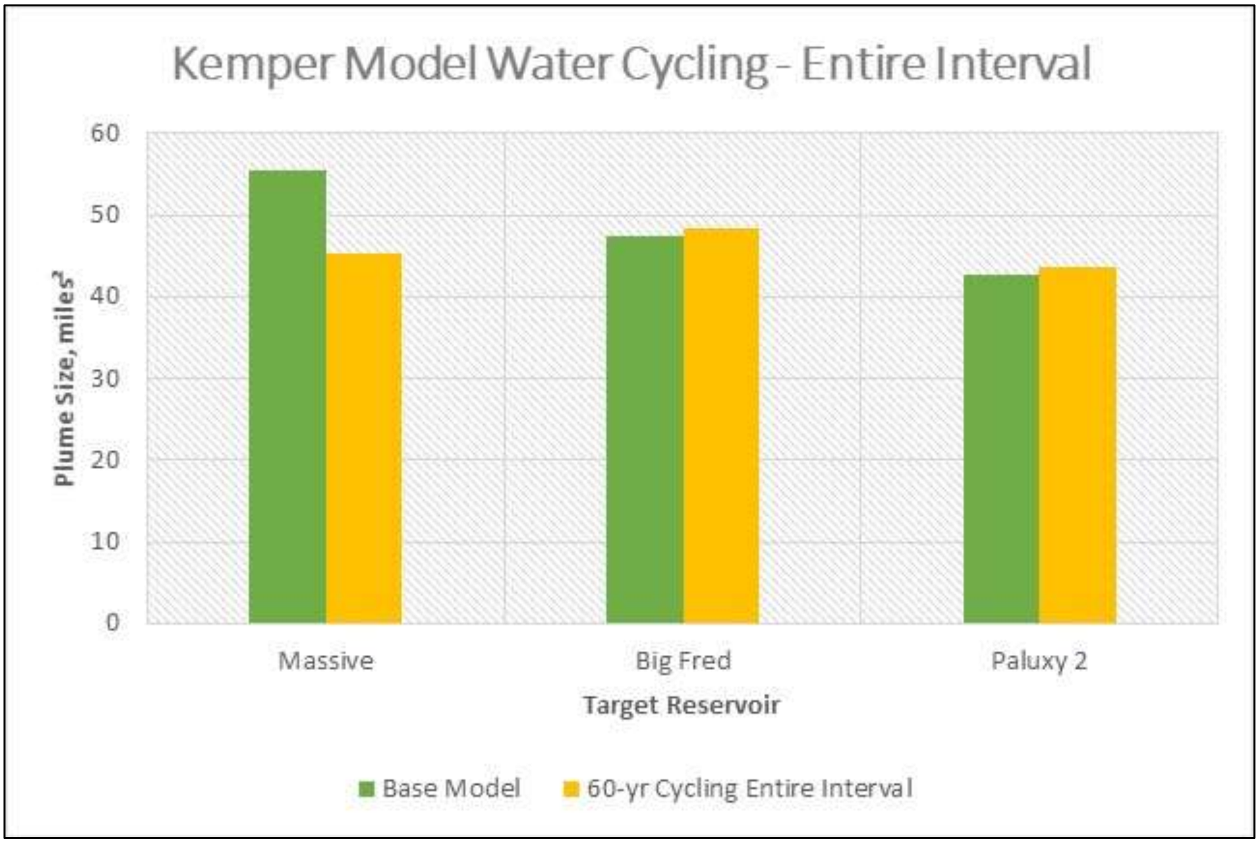

Figure 20: Impact of water cycling on plume size. Water injection wells are perforated through the entire reservoir interval

Figure 21 shows the CO_2 saturation at the top of the Massive Sand formation at the end of 60-year simulation. The overall impact of this cycling case was a plume size reduction of about 18%, which occurred in the Massive Sand.

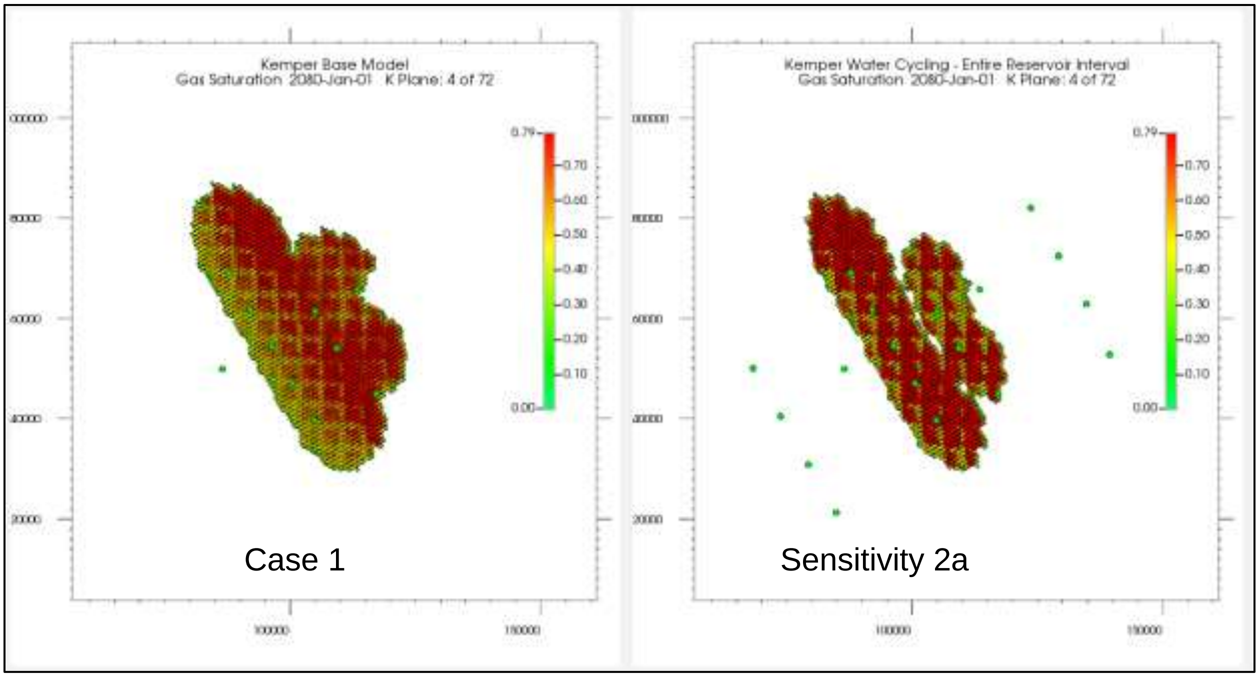

Figure 21: Kemper water cycling (Sensitivity 2a). Plume size at the top of Massive Sand

In the next well configuration scenario (Sensitivity 2b), the water injection wells are placed on the Northwest of the injection area whereas the water extraction wells are placed on the Southeastern side of the injection site (**Figure 22**).

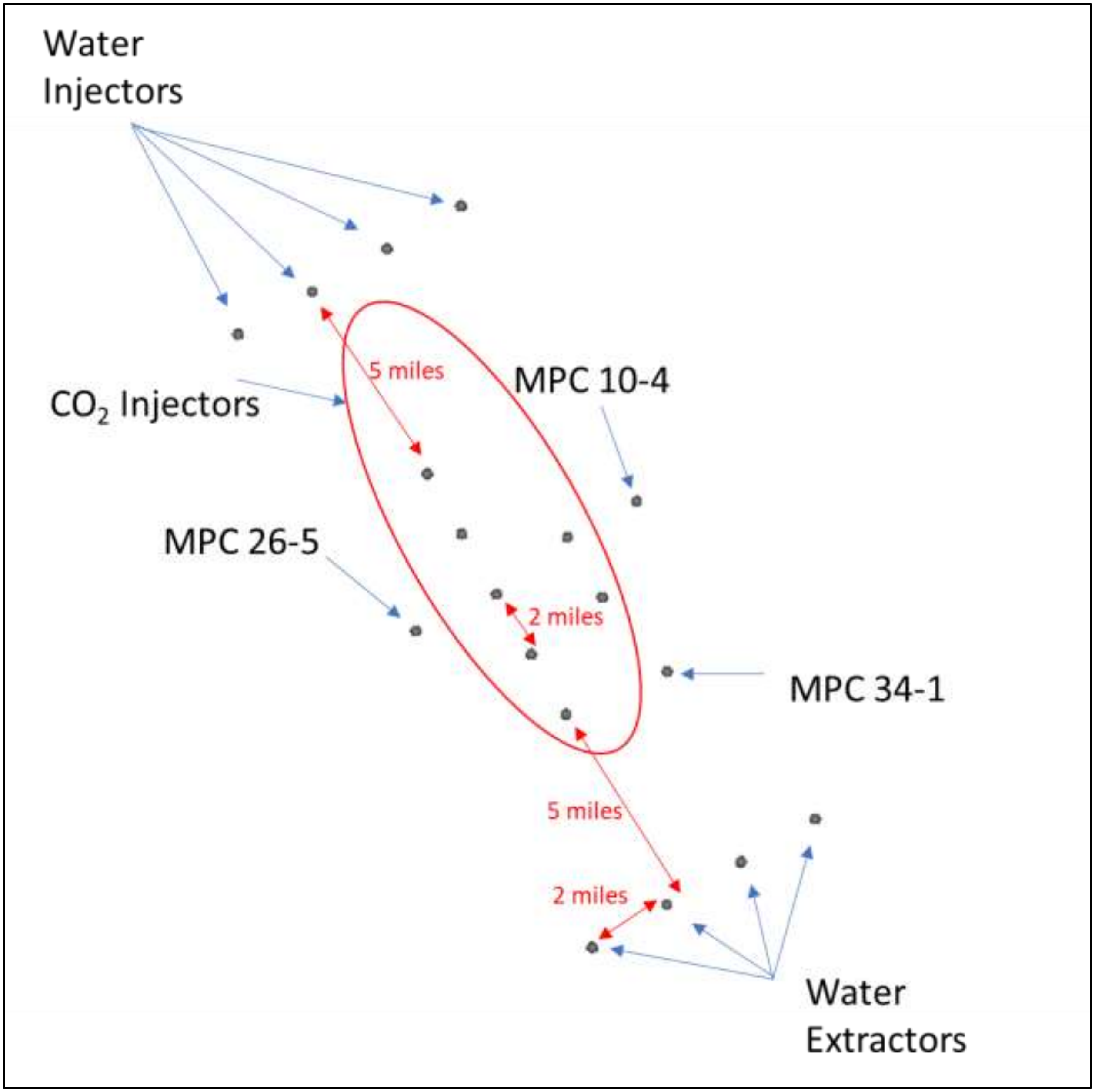

Figure 22: Water cycling wells location (Sensitivity 2b) map

In this scenario, the water injection wells are perforated in only the top 5 layers (about 100 feet) of each target reservoir. As it is shown on **Figure 23**, the CO_2 plume tends to move Southeast, towards the water extraction wells. This well configuration did not have an impact on plume size (54 square miles vs 55 square miles, which is essentially the same).

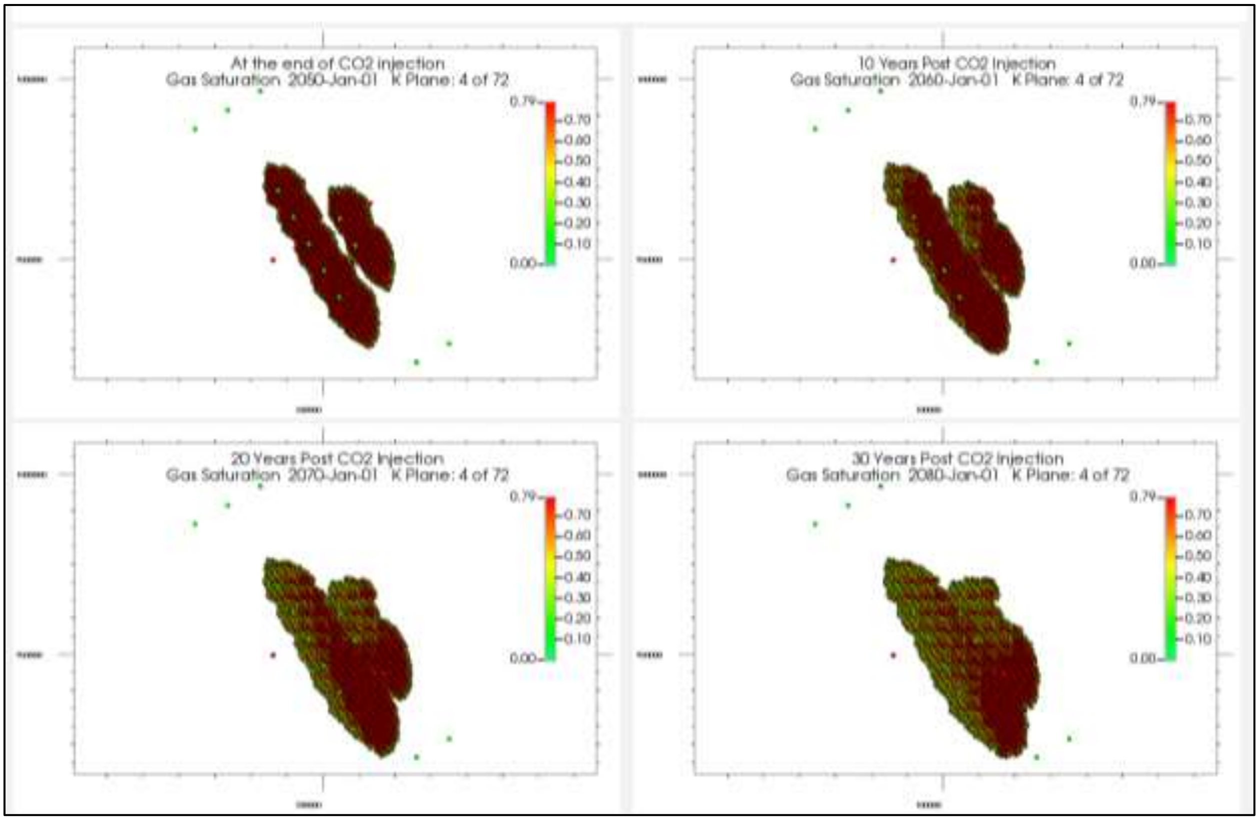

Figure 23: Impact of water cycling (Sensitivity 2b) on CO_2 plume

Another well location scenario (Sensitivity 2c) was to consider placing two wells on each of the four sides of the CO_2 injection site. The four wells (two on each opposite side of the CO_2 injection site) along the high permeability direction in the Northwest-Southeast direction were selected as water injectors. Water extractors were placed on the Southwest-Northeast direction along the dip of the formation and the lower horizontal permeability direction. **Figure 24** shows this well configuration. The water extractors were placed 5 miles away from the closest CO_2 injection well, while the water injectors were placed closer to the CO_2 injection site at 3 miles. The water injectors were again perforated in the top about 100 feet of the Massive Sand, Big Fred, and Paluxy 2, while the water extractors were perforated throughout these formations. CO_2 was still being injected through the entire interval of the three reservoir groups.

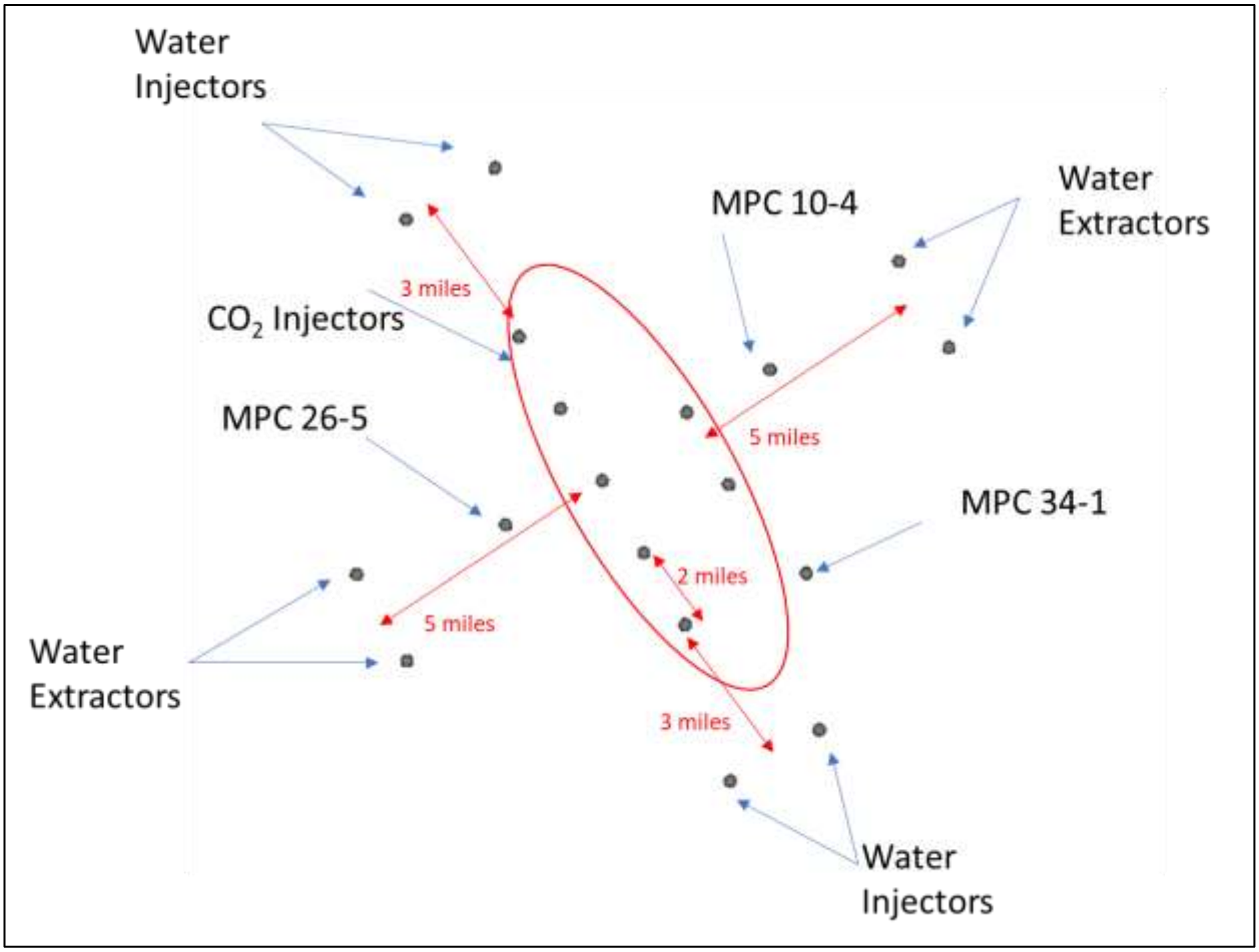

Figure 24: Water cycling wells location (Sensitivity 2c) map

This well configuration along with limited perforation interval in the water injection wells resulted in 5% reduction in the CO_2 plume size, which occurred at the top of the Massive Sand formation. **Figure 25** shows the gas saturation at the top of the Massive Sand formation. The maps on the figure show the CO_2 plume advancement through time. From left to right and top to bottom, the maps show the gas saturation distribution at the end of CO_2 injection, 10 years, 20 years, and 30 years post CO_2 injection.

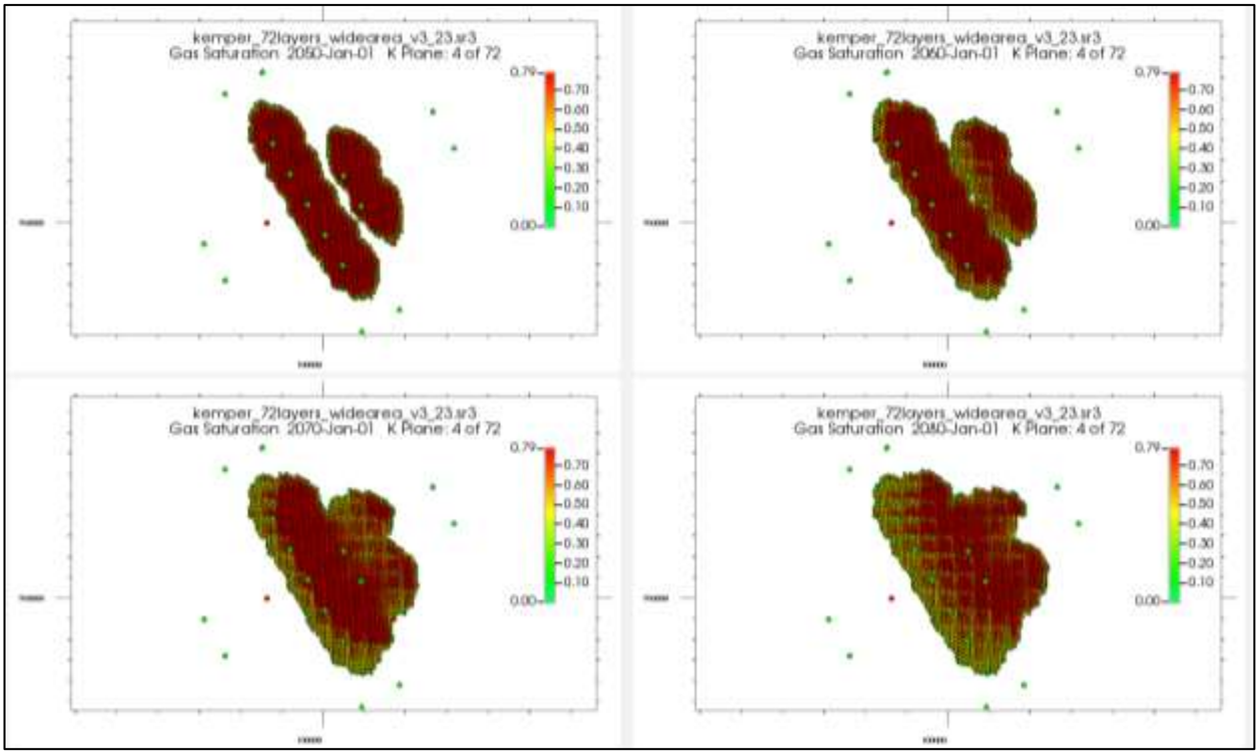

Figure 25: Impact of water-cycling wells' location (scenario 2c) on CO2 plume migration

5.3 Sensitivity Analysis – Water Injector Wells' Perforation Interval (Sensitivity 3)

A case (Sensitivity 3) was built in which the water injection wells were perforated only at the top about 100 feet of each target formation. Like the full-interval perforation case, the water extraction wells were perforated in the entire interval of the target reservoirs. **Figure 26** shows the comparison of the plume size at the top of the Massive Sand formation for the two perforation schemes. It was observed that the partial-perforation interval had a smaller impact on plume size reduction (10%) when compared to 18% reduction in the case of full-interval perforation.

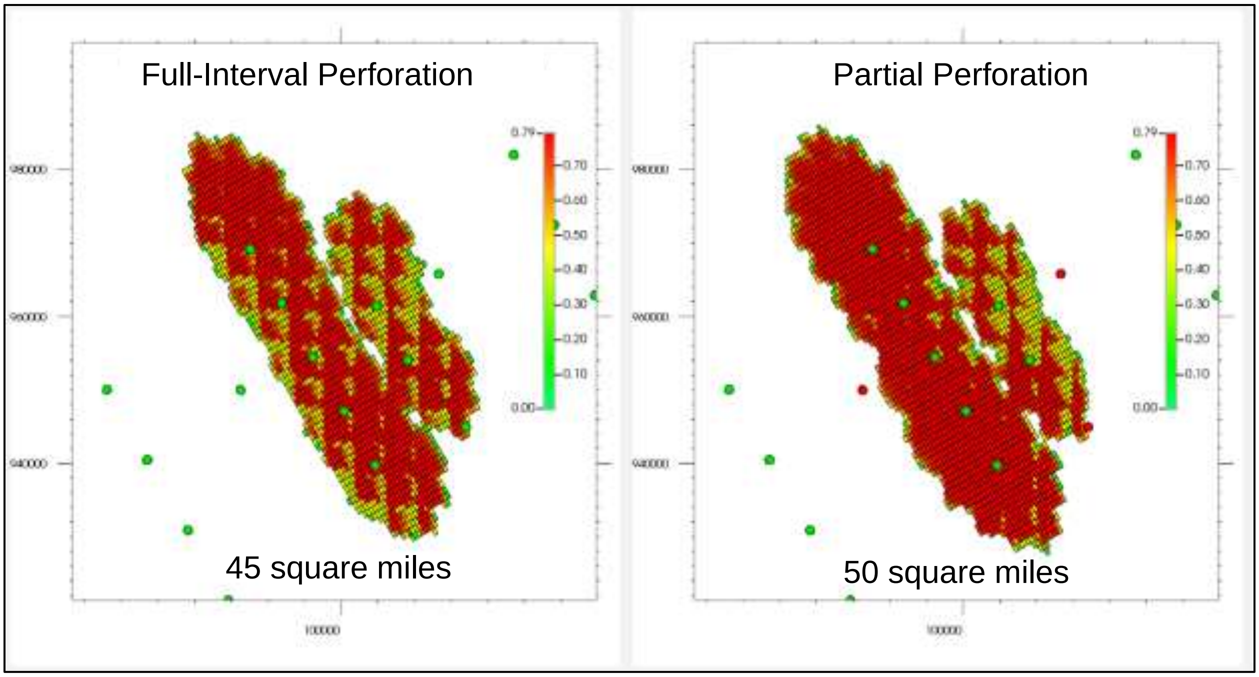

Figure 26: CO_2 gas saturation map to showing the impact of perforation interval in the water injections.

5.4 Sensitivity Analysis – Hysteresis Residual Gas Saturation (Sgrmax) (Sensitivity 4)

Three additional cases were run to test the sensitivity of the plume size to Sgrmax. The cases assumed the values of 5.1% (Sensitivity 4a), 15% (Sensitivity 4b), and 40% (Sensitivity 4c) and all included 60 years of water cycling. As a reminder, the base case Sgrmax is 15%. **Figure 27** shows the gas saturation distribution at the top of Massive Sand at the end of the 60-year simulation time. The map on the top left shows the CO_2 plume for the base case. The top-right map shows the CO_2 plume for a water cycling case where Sgrmax was assumed to be 5.1%. The bottom-left map is the result of a 60-yr water cycling case assuming Sgrmax of 15%. Finally, the bottom-right map is for the case with Sgrmax of 40%. Increasing the Sgrmax value from 5.1% to 40% causes a 5% decrease in the plume size, from 46 square miles to 43 square miles.

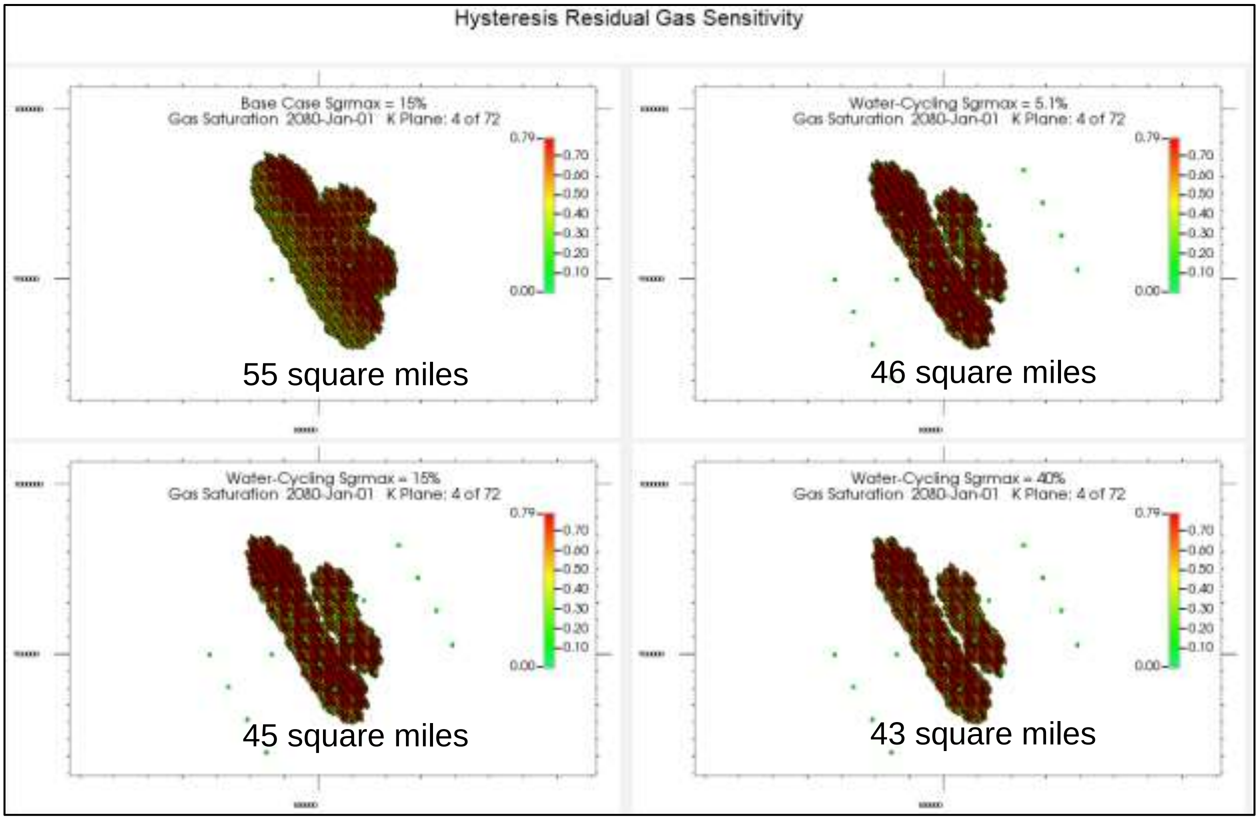

Figure 27: Testing the effect of hysteresis residual gas saturation on gas trapping and CO_2 plume movement

The summary of the results is provided in **Table 8** below.

Table 8: Kemper modelling results summary

Model	Kh Anisotropy	Kv/Kh_avg	Hysteresis Sgrmax (%)	Total CO_2 Injected, (MMmt)	Total Water Injected (STB)	Water Injector Perforation	Plume Size (square miles)
Case 1	3:1	1:10	15	675	-	-	55
Sensitivity 1	1:1	1:10	15	675	-	-	70
Sensitivity 2a	3:1	1:10	15	675	5.26E+9	Full interval	45
Sensitivity 2b	3:1	1:10	15	675	5.26E+9	Top 100 feet	54
Sensitivity 2c	3:1	1:10	15	675	5.26E+9	Top 100 feet	53
Sensitivity 3	3:1	1:10	15	675	5.26E+9	Top 100 feet	50
Sensitivity 4a	3:1	1:10	5.1	675	5.26E+9	Full interval	46
Sensitivity 4b	3:1	1:10	15	675	5.26E+9	Full interval	45
Sensitivity 4c	3:1	1:10	40	675	5.26E+9	Full interval	43

6.0 Conclusions

Large volume injection and storage of CO_2 in vertically-stacked saline formations in the Kemper Regional Storage Complex was studied through reservoir flow simulation. A base model was developed using the latest geologic interpretation at the Kemper CO_2 Storage Complex in Kemper County, Mississippi. The simulation results from the base case show that injecting a total volume of 675 million metric tons of CO_2 over 30 years is attainable, and the CO_2 is contained within the target formations in an area of approximately 55 square miles. Due to limited data availability to determine permeability anisotropy and hysteresis trapping, sensitivity analysis was performed to test the impact of these parameters on the plume migration and its extent. Horizontal permeability anisotropy has the largest impact on the plume size. Lack of permeability anisotropy causes the CO_2 plume to cover about 70 square miles at the top of the Massive Sand. This is approximately 27% higher than the base case, where a 3:1 horizontal permeability anisotropy was used. During phase III of this project, special attention will be given to evaluating the horizontal permeability anisotropy ratio and the direction of the higher permeability. Additional observation wells around the storage site would provide valuable information on CO_2 movement and better estimating the permeability anisotropy through reservoir simulation and history matching.

A summary of the results from the simulation study is presented here.

- An isotropic horizontal permeability case will result in a 70 square mile plume, approximately 27% larger than the base case (3:1 horizontal permeability anisotropy).
- A change of hysteresis residual gas saturation from 5.1% to 40% (in a water-cycling scenario) results in a 5% change in the CO_2 plume size (from 17% to 22%). A water-cycling scenario with a 15% Sgrmax (similar to the base case), resulted in 18% reduction in the plume size compared to the base case.
- Changing the perforation interval of the water injectors from perforating the entire target reservoir interval to only the top roughly 100 feet of the target formation results in the plume size reduction of 10% in the case of partial perforation and 18% in the case of full-interval perforation, compared to the base case
- Placing the water injection wells up-dip of the CO_2 injection site (northeast) with full-interval perforation and water extraction wells down-dip of the CO_2 injection site (southwest) results in an 18% plume reduction

7.0 References

Advanced Resources International. (2015). *Southeast Carbon Sequestration Partnership (SECARB) Phase III Anthropogenic Test at Citronelle Field, Mobile Co., AL.* Arlington, VA: Advanced Resources International.

Advanced Resources International. (2016). *Southeast Carbon Sequestration Partnership (SECARB) Phase III Anthropogenic Test at Citronelle Field, Mobile Co., AL.* Arlington, VA: Advanced Resources International.

Advanced Resources International. (2020). *Geological Framework Report, Special Topical Report.* Arlington, VA.

Akbarabadi, M., Arshadi, M., & Khishvand, M. (2019). *Steady-state CO2/Brine Relative Permeability Measurements.* Laramie, WY: PIRI Technologies, LLC.

Berg, S., Oedai, S., & Ott, H. (2011). *Unsteady-State CO2-Brine Displacement in Sandstone: Relative Permeability and Mass Transfer for Saturated and Unsaturated Phases.* France: Les Rencontres Scientifiques d'IFP Energies Nouvelles.

Huval, R. (2018). *Water Analysis, Well No. MPC 34-1 Kemper County, Mississippi, Report No. 201801231-5018058379.* Broussard, Luisiana: Reservoir Fluid Services.

Huval, R. (2019). *Water Analysis, MPC 10-4, Kemper County, Mississippi, Report No. 201901859-5019088302.* Broussard, Luisiana: Reservoir Fluid Services.

Jalali, J. (2019). *Well 10-4 Well Test Interpretation.*

Levine, J. (2011). *Relative Permeability Experiments of Carbon Dioxide Displacing Brine and Their Implications for Carbon Sequestration.* New York: Columbia University.

Pashin, J. et al.. The Paluxy Formation in the East-Central Gulf of Mexico Basin: geology of a giant anthropogenic CO2 sink. AAPG 2018 Annual Convention and Exposition

Folaranmi, A. T., 2015, Geologic characterization of a saline reservoir for carbon sequestration: The Paluxy Formation, Citronelle Dome, Gulf of Mexico Basin, Alabama: Stillwater, Oklahoma State University, unpublished Master's thesis, 96 p.

Allen, J.R.L., 1978. Studies in fluviatile sedimentation: an exploratory quantitative model for the architecture of avulsion-controlled alluvial suites. Sedimentary Geology 21: 129-147

King, P.R., 1990, The connectivity and conductivity of overlapping sand bodies; North Sea oil and gas reservoirs; II, Proceedings of the North Sea oil and gas reservoirs conference, in 2nd North Sea oil and gas reservoirs conference, May 8-11, 1989, Trondheim, Norway: United Kingdom (GBR), Graham & Trotman, London, United Kingdom (GBR).

Allard D., Heresim Group (1993) On the Connectivity of Two Random Set Models: The Truncated Gaussian and the Boolean. In: Soares A. (eds) Geostatistics Tróia '92. Quantitative Geology and Geostatistics, vol 5. Springer, Dordrecht

Pashin, J. C., Hills, D. J., Kopaska-Merkel, D. C., and McIntyre, M. R., 2008, Geological evaluation of the potential for CO_2 sequestration in Kemper County, Mississippi: Final Report, Southern Company Contract 8-08-00142, 53 p.

Frascogna, X. M., editor, 1957, Mesozoic-Paleozoic producing areas of Mississippi and Alabama: Mississippi Geological Society, v. I, 139 p.

Davis, D. C., and Lambert, E. H., Jr., editors, 1963, Mesozoic-Paleozoic producing areas of Mississippi and Alabama: Mississippi Geological Society, v. II, unpaginated.

Galicki, S. J., editor, 1986, Mesozoic-Paleozoic producing areas of Mississippi and Alabama: Mississippi Geological Society, v. III, unpaginated.

Pashin, J. C., Raymond, D. E., Alabi, G. G., Groshong, R. H., Jr., and Guohai Jin, 2000, Revitalizing Gilbertown oil field: Characterization of fractured chalk and glauconitic sandstone reservoirs in an extensional fault system: Alabama Geological Survey Bulletin 168, 81 p.